

The University of Maine

DigitalCommons@UMaine

---

Electronic Theses and Dissertations

Fogler Library

---

Spring 5-6-2022

## Development of a Structural Finite Element Modeling Approach for Hybrid Composite-Steel Shipping Containers

Jason Nagy  
jason.nagy@maine.edu

Follow this and additional works at: <https://digitalcommons.library.umaine.edu/etd>



Part of the [Mechanical Engineering Commons](#)

---

### Recommended Citation

Nagy, Jason, "Development of a Structural Finite Element Modeling Approach for Hybrid Composite-Steel Shipping Containers" (2022). *Electronic Theses and Dissertations*. 3593.  
<https://digitalcommons.library.umaine.edu/etd/3593>

This Open-Access Thesis is brought to you for free and open access by DigitalCommons@UMaine. It has been accepted for inclusion in Electronic Theses and Dissertations by an authorized administrator of DigitalCommons@UMaine. For more information, please contact [um.library.technical.services@maine.edu](mailto:um.library.technical.services@maine.edu).

**DEVELOPMENT OF A STRUCTURAL FINITE ELEMENT MODELING APPROACH  
FOR HYBRID COMPOSITE-STEEL SHIPPING CONTAINERS**

By

Jason Louis Nagy

B.S. University of Maine, 2020

A THESIS

Submitted in Partial Fulfillment of the

Requirements for the Degree of

Master of Science

(in Mechanical Engineering)

The Graduate School

The University of Maine

May, 2022

Advisory Committee:

Dr. Anthony Viselli, Chief Engineer, Ocean Engineering and Energy, Assistant Research  
Professor of Civil Engineering, Co-Advisor

Dr. Andrew Goupee, Associate Professor of Mechanical Engineering, Co-Advisor

Dr. Robert Lindyberg, Graduate External Faculty of Civil Engineering

© 2022 Jason L. Nagy

All Rights Reserved

# **DEVELOPMENT OF A STRUCTURAL FINITE ELEMENT MODELING APPROACH FOR HYBRID COMPOSITE-STEEL SHIPPING CONTAINERS**

By Jason Louis Nagy

Thesis Advisors: Anthony Viselli, Andrew Goupee

An Abstract of the Thesis Presented  
in Partial Fulfillment of the Requirements for the  
Degree of Master of Science  
(in Mechanical Engineering)  
May 2022

This thesis presents a summary of the development and verification of structural finite element (FE) models for predicting key responses of ISO composite-steel shipping containers. The container has a steel perimeter frame with composite corrugated panels bonded to steel tabs welded to the frame. This thesis presents the development of the FE models to predict structural behavior when the container undergoes select International Standards Organization standard 1496-1 structural tests. Composite and steel mechanical properties were predicted and matched to measured data from coupon tests. Individual panels were modeled and matched to individual three-point bending tests. The individual panel models were developed into partial container models for the sidewall strength test, roof strength test, frontwall strength test and fork-lift pocket lifting test. Then the models were compared and verified against full-scale test data. The FE models include geometric and material non-linearity capability to successfully predict extreme loads on the container. This thesis serves as a milestone in the hybrid composite-steel shipping container modeling process and will be used for developing FE models for other container variations.

## **ACKNOWLEDGMENTS**

I would like to thank everyone who has worked on this research project over the past two years. I would not be able to present this thesis without their help. I would like to thank my committee members for the experience and help they gave; Dr. Anthony Viselli, Dr. Andrew Goupee and Dr. Robert Lindyberg. I would like to thank Thomas Snape for being part my weekly update meetings. I would like to thank my parents, Jim and Lynn Nagy, for giving me their full support through undergrad and graduate school. Emily Pierce cannot go unmentioned with her support while I was writing and revising this thesis. I would like thank everyone who helped setup and run the full-scale testing. Lastly, I would like to thank Thomas Snape, Robert Michaud and Peter Smith for always sending me the data I needed.

This thesis is based upon work supported by the United States Air Force, under Contract No. FA8650-19-2-5503. Any conclusions, findings, or recommendations expressed in this thesis are those of the author and do not necessarily reflect the views of the United States Air Force.

## TABLE OF CONTENTS

AKNOWLEDGMENTS .....	iii
LIST OF TABLES .....	vi
LIST OF FIGURES .....	vii
1 INTRODUCTION .....	1
1.1 Research Plan .....	1
1.2 Overview of Hybrid Composite-Steel Container and Structures .....	2
1.3 ISO Required Testing .....	4
2 LAMINATE ANALYSIS AND COMPARISON WITH TESTING DATA.....	5
2.1 VectorLam.....	5
2.2 Coupon Comparison.....	6
2.2.1 Gen1 Laminate Comparison .....	8
2.2.2 Gen2 Laminate Comparison .....	12
2.3 Generation Comparison.....	13
3 FINITE ELEMENT ANALYSIS OF INDIVIDUAL PANELS .....	15
3.1 Three-Point Bending Tests.....	15
3.2 Ansys Three-Point Bending Test Models .....	18
4 FULL-SCALE CONTAINER FINITE ELEMENT MODELS.....	23
4.1 Steel Verification.....	23
4.2 Sidewall Strength Test .....	25
4.2.1 Development of Ansys Sidewall Strength Test Model.....	28
4.2.2 Comparison of Full-Scale Test Data to Ansys Data .....	33
4.2.3 Model Conclusions .....	37

4.3	Roof Strength Test .....	37
4.3.1	Development of Ansys Roof Strength Test Model.....	39
4.3.2	Comparison of Full-Scale Test Data to Ansys Data .....	40
4.3.3	Modeling Conclusions .....	40
4.4	Frontwall Strength Test.....	41
4.4.1	Development of Ansys Frontwall Strength Test Model .....	44
4.4.2	Comparison of Full-Scale Test Data to Ansys Data .....	45
4.4.3	Modeling Conclusions .....	48
4.5	Lifting From Fork-Lift Pockets Test.....	48
4.5.1	Development of Ansys Fork Pocket Lift Test Model.....	50
4.5.2	Comparison of Full-Scale Test Data to Ansys Data .....	53
4.5.3	Modeling Conclusions .....	54
5	CONCLUSIONS AND POTENTIAL IMPLEMENTATIONS.....	55
5.1	Conclusions .....	55
5.2	Potential Implementations.....	56
	REFERENCES .....	57
	APPENDIX A: ATTACHMENTS.....	58
	APPENDIX B: THREE-POINT BENDING TEST PLOTS .....	60
	BIOGRAPHY OF THE AUTHOR.....	64

## LIST OF TABLES

Table 1: Gen1 and Gen2 Laminate Layups for Individual Panels.....	7
Table 2: Gen1 Matched VectorLam MOE to As Built MOE in the 1-Direction.....	8
Table 3: Measured to Predicted Fabric Weight Comparison.....	9
Table 4: Initial to Final Predicted Fabric Weight Comparison.....	9
Table 5: Gen1 Comparison of VectorLam to As Built Physical and Mechanical Properties.....	10
Table 6: Gen1 Door Panel Extra Physical and Mechanical Properties.....	11
Table 7: Gen2 Matched VectorLam MOE to As Built MOE in the 1-Direction.....	12
Table 8: Gen2 Comparison of VectorLam to As Built Physical and Mechanical Properties.....	13
Table 9: Comparison of Gen2 to Gen1 Predicted Key Properties .....	14
Table 10: Three-Point Bending Test and Ansys Maximum Load Deflection Data.....	22
Table 11: Comparison of Sidewall Strength Test Mid-Span Deflection .....	34
Table 12: Comparison of Sidewall Full Test Load Strains.....	36
Table 13: Comparison of Roof Strength Test Position 7.4 Center Deflection .....	40
Table 14: Comparison of Frontwall Strength Test Mid-Span Deflection.....	46
Table 15: Comparison of Frontwall Strength Test Strains .....	47
Table 16: Comparison of Fork Pocket Test Corner Post Deflection .....	53
Table 17: Comparison of Fork Pocket Test Strains .....	53



## LIST OF FIGURES

Figure 1: Standard Steel Container .....	2
Figure 2: The University of Maine Hybrid Container Steel Frame Components.....	2
Figure 3: The University of Maine Hybrid Composite-Steel Container .....	3
Figure 4: VectorLam Gen1 Sample Output .....	6
Figure 5: Primary Direction of Bending of Panels .....	10
Figure 6: Three-Point Bending Test Schematic with Sidewall Panel.....	15
Figure 7: Door Panel Three-Point Bending Test Loaded .....	16
Figure 8: Roof Panel Three-Point Bending Test Loaded.....	16
Figure 9: Sidewall Panel Three-Point Bending Test Loaded.....	17
Figure 10: Frontwall Panel Three-Point Bending Test, Unloaded (Left), Loaded (Right).....	17
Figure 11: Door Panel, Three-Point Bending Test Ansys Setup .....	18
Figure 12: Roof Panel, Three-Point Bending Test Ansys Setup .....	19
Figure 13: Sidewall Panel, Three-Point Bending Test Ansys Setup .....	20
Figure 14: Frontwall Panel, Three-Point Bending Test Ansys Setup.....	21
Figure 15: Steel Coupon Tensile Test Setup.....	23
Figure 16: Steel Coupon Tensile Test Ansys Setup.....	24
Figure 17: Comparison of Test and Ansys Steel Coupon Stress-Strain Curves .....	25
Figure 18: ISO 1496 Annex A Figure A.8.....	26
Figure 19: Sidewall Strength Test Setup .....	26
Figure 20: Sidewall Strength Test Loaded.....	27
Figure 21: String Pot Locations on the Sidewall .....	27
Figure 22: Strain Gauge Locations on the Sidewall .....	28

Figure 23: Sidewall Strength Test Version 1 Model Boundary Conditions .....	29
Figure 24: Sidewall Strength Test Version 1 with Unit Pressure Applied .....	30
Figure 25: Sidewall Strength Test Version 2 .....	30
Figure 26: Sidewall Strength Test Version 2 Concrete Block Load.....	31
Figure 27: Sidewall Strength Test Version 3 .....	32
Figure 28: Version 3 Deflection Contour Plot for Concrete Block Load .....	32
Figure 29: Sidewall Model Mesh Convergence Study .....	33
Figure 30: ISO 1496-1 Annex A Figure A.9 .....	38
Figure 31: Roof Strength Test Setup .....	38
Figure 32: Roof Strength Test Load Positions.....	39
Figure 33: Roof Strength Test BC and Load .....	39
Figure 34: ISO 1496-1 Annex A Figure A.7 .....	41
Figure 35: Frontwall Strength Test Setup.....	42
Figure 36: Frontwall Strength Test Loaded .....	43
Figure 37: Strain Gauge Locations on the Frontwall.....	43
Figure 38: Frontwall Model Load and Initial BC .....	44
Figure 39: Frontwall Model Load and BC.....	45
Figure 40: Fork Pocket Test Setup.....	49
Figure 41: Fork Pocket Test String Pot Locations.....	49
Figure 42: Fork Pocket Test Fixtures.....	50
Figure 43: Fork Pocket Test Version 1 BC.....	51
Figure 44: Version 1 Y-Deflection Contour Plot.....	51
Figure 45: Fork Pocket Test Version 2 BC.....	52

## CHAPTER

### 1 INTRODUCTION

This thesis presents an overview of important structural responses, full-scale testing, and the development of finite element analysis (FEA) modeling techniques useful for assessing structural behavior of hybrid composite-steel shipping containers during International Standards Organization (ISO) standard 1496-1 structural testing. The containers conform to ISO standard 668. This work was funded by Global Secure Shipping (GSS) under an award from the United States Air Force. The goal of this research was to develop practical FEA techniques and models of a hybrid composite-steel ISO compliant container, constructed with polymer matrix composite materials and adhesive joints. This thesis presents the development of FEA models and techniques used to predict hybrid composite-steel containers important structural responses.

#### 1.1 Research Plan

The development of the FEA models starts with identifying important structural responses to predict whether the container will pass structural testing requirements per ISO 1496-1. Full-scale structural test data of a standard steel container per ISO 1496-1 collected by the Advanced Structures and Composites Center (ASCC) was used to determine key structural responses including deflection and strain at various points within the container. The data was used to understand the behavior of the container under the ISO loading to inform the model development process.

Next, composite coupon tensile tests were conducted at the ASCC for comparison to predicted laminate models, to ensure that the proper input data is used. The laminate models were implemented into Ansys, the FEA tool used for all modeling in this research. Next, the testing and modeling of individual panels to identify appropriate modeling techniques for ISO

testing was conducted. Development of subassemblies and full container FEA models and validating through full-scale ISO structural test data. Finally, implementing the FEA models to inform further design modifications to minimize weight.

## 1.2 Overview of Hybrid Composite-Steel Container and Structures

Hybrid composite-steel containers are similar in overall design to standard steel ISO containers. See Figure 1 for a steel container with the panels labeled (20FT. Containers) and Figure 2 (Viselli, 2006) for the steel frame.



Figure 1: Standard Steel Container

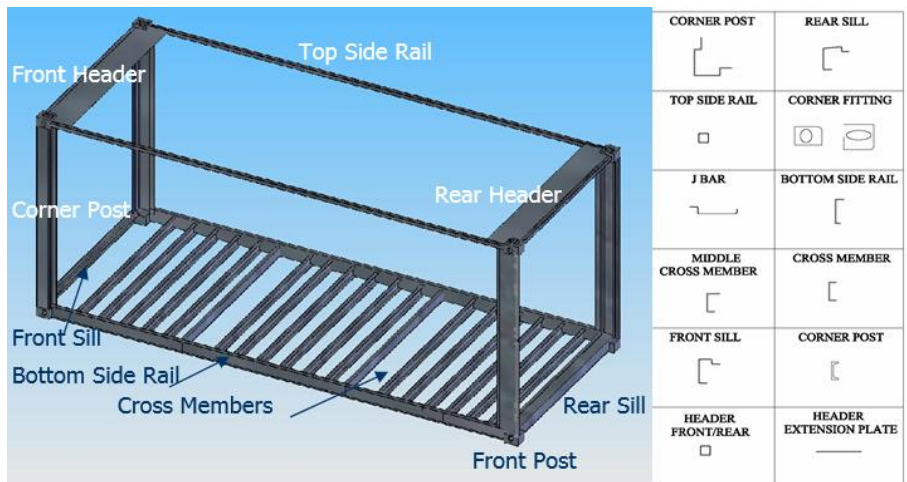


Figure 2: The University of Maine Hybrid Container Steel Frame Components

Steel containers are widely used around the world for transporting cargo by truck, train and sea. They have been standardized for convenience but can be modified; however, it must always satisfy the structural requirements of ISO 1496-1.

In recent years composites have been used to shed weight off of high-end automobiles and aircrafts. Key components such as the frame are typically kept as steel, while the doors and body could be made from carbon-fiber composites. A composite is typically a high performance fabric in a matrix material that combine together to provide enhanced properties compared to the individual materials alone. Prior to this research the University of Maine researched the feasibility of introducing composites into containers. The research led to the production of a hybrid composite-steel container full-scale prototype. The steel ceiling, doors, sidewalls and frontwall were swapped for composites, while the frame remained steel. See Figure 3 for the prototype (Viselli, 2006).



Figure 3: The University of Maine Hybrid Composite-Steel Container

The container follows the ISO type 1CC container dimensions of 20 ft long with a height of 8.5 ft and 8 ft wide. The composite panels are encompassed and bonded to steel tabs with adhesive

which are then welded into the frame. This researched container starts with generation one (Gen1) laminate layups, which then get refined into generation two (Gen2) laminate layups through small and full-scale testing. See Table A 1 row 1 for container and test setup drawings.

### **1.3 ISO Required Testing**

Design standards for containers are set by the ISO. These standards must be followed in order for a container to be used in the intermodal supply chain. ISO 1496-1 structural test loads for a container are based off its rating define by ISO, tare and maximum payload (P), which is its tare subtracted from the rating. For the containers tested in this research the P equals 62,600 lb. The containers materials are not specified, but all containers must pass the structural requirements of ISO 1496-1 which references ISO 1161, dimension requirements of the corner castings, and ISO 668, dimension requirements of the container. ISO 1496-1 requires a container to pass structural tests that simulate extreme conditions the container may undergo during transport: stacking, racking, wall bending, floor loading and lifting tests. In depth explanations of the relevant structural tests will be presented in Chapter 4.

## CHAPTER

### 2 LAMINATE ANALYSIS AND COMPARISON WITH TESTING DATA

This chapter presents the laminate analysis model used to predict mechanical and material properties of the composite wall panels. The manufactured panels are produced through light resin transfer molding, which typically produces a lower mass fraction than a vacuum infusion process. The laminate analysis model was verified against experimental coupon mechanical test data and outputs gross mechanical properties to be used within the FEA model. In this project, a software called VectorLam was implemented to predict the remaining data needed to completely define the FEA models.

#### 2.1 VectorLam

VectorLam predicts physical properties such as, but not limited to, thickness, weight, and volume fraction. It also predicts mechanical properties such as, but not limited to, elastic modulus in the fiber and transverse directions, stiffness, and tensile and compressive strength (Vectorply, n.d.).

VectorLam has a comprehensive library of laminas and allows the user to define their own. It allows different laminate layups to be created, while changing layer properties. The reporting feature is shown with sample Gen1 layups in Figure 4.

		C2 Door	C3 Roof	C3 Side Wall	C3 FWR	C3 FWR
Layer	1	C2 E-M 0015	C2 E-M 0015	C2 E-M 0015	C2 E-M 0015	C2 E-M 0015
	2	C2 CFM 0015	C2 CFM 0015	C2 CFM 0015	C2 CFM 0015	C2 CFM 0015
	3	C2 E-LR 1208	C3 E-LR 1708	C3 SW-VT-280	C3 E-LR 2410	C3 E-LR 2410
	4	C2 VT-280	C2 Roof-VT-280	C3 SW-VT-280	C3 E-LR 2410	C3 E-LR 2410
	5	C2 Soric SF 2	C2 Soric SF 2	C3 SW-VT-280	C3 E-LR 2410	C3 E-LR 2410
	6	C2 VT-280	C2 Roof-VT-280	C2 Soric SF 2	C3 Soric SF 2	C3 Soric XF 4
	7	C2 E-LR 1208	C3 E-LR 1708	C3 SW-VT-280	C3 E-LR 2410	C3 E-LR 2410
	8	C2 CFM 0015	C2 CFM 0015	C3 SW-VT-280	C3 E-LR 2410	C3 E-LR 2410
	9	C2 E-M 0015	C2 E-M 0015	C3 SW-VT-280	C2 CFM 0015	C3 E-LR 2410
	10			C2 CFM 0015	C2 E-M 0015	C3 E-LR 2410
	11			C2 E-M 0015		C2 CFM 0015
	12					C2 E-M 0015
Total Wt.	lb/ft <sup>2</sup>	2.12	2.34	2.79	2.66	2.93
Thickness	in	0.292	0.321	0.366	0.366	0.410
0° Modulus, Ex	Msi	2.204	2.257	3.32	2.526	2.845
90° Modulus, Ey	Msi	1.103	1.081	1.47	1.076	1.130
Shear Modulus, Gxy	Msi	0.427	0.421	0.68	0.441	0.475
0° Flex. Stiffness	lb-in <sup>2</sup> /in	4,161.23	5,661.34	10,965.8	8,938.04	19,944.97
90° Flex. Stiffness	lb-in <sup>2</sup> /in	2,710.76	3,506.22	5,623.41	4,061	8,999.63
0° Ten. Ult. Stress	ksi	13,226	13,543	19,929	11,742	14,214
90° Ten. Ult. Stress	ksi	6,618	6,483	8,522	6,448	5,646
0° Comp. Ult. Stress	ksi	8,817	9,029	13,286	10,000	28,428
90° Comp. Ult. Stress	ksi	4,412	4,322	5,681	4,200	11,293
Shear Ult. Stress	ksi	5,123	5,066	6,799	5,304	4,764
VF	%	36.3	37.8	48.0	38.8	50.9
WF	%	47.6	46.7	59.7	48.9	57.2
Poisson Ratio, PRxy		0.27	0.27	0.25	0.28	0.27
0° Ult. B. Moment	in lb/in	699	867	1,600	1,187	2,020
90° Ult. B. Moment	in lb/in	455	538	818	669	939

Data for comparative purposes only

Figure 4: VectorLam Gen1 Sample Output

The name of the laminate is shown at the top, with its corresponding layup shown directly below in its laid-up order. The layer number is shown on the far left. Below the layer numbers are the desired properties selected with their corresponding units. To the right of the properties are the laminate values for the property in that row. The thickness, moduli and Poisson's ratio are critical properties when developing the FEA models. These critical properties along with the total weight and mass fraction are critical for assessing the accuracy of the prediction. See Table A 1 row 2 and 3 for VectorLam Gen1 and Gen2 outputs, respectively.

## 2.2 Coupon Comparison

Table 1 shows the Gen1 and Gen2 laminate layups for individual panels. The door panel layups are shown in the upper left, the roof panel layups in the upper right, the sidewall panel layups in the lower left and the frontwall panel layups in the lower right. The frontwall Gen1 panel is reinforced in the center of the wall, and its layup is called Gen1 – Center. It is a 16 inch section parallel to the corrugations and centered in the panel.



The individual material layers have different functions. The stitchmat layers have randomly oriented fibers and hold the layup together for easier manufacturing. The CFM layers are continuous fiber mats that provide bi-axial support. The E-LR and VT layers provide support in the 1-direction. The soric layers are cores and allow for more even resin distribution. The E-BX layers provide shear support with a +45/-45 fabric layup.

Table 1: Gen1 and Gen2 Laminate Layups for Individual Panels

Door		
Layer	Gen1	Gen2
1	Stitchmat - 1.5 oz	Stitchmat - 1.5 oz
2	CFM 0015	CFM 0015
3	E-LR 1208	VT 280
4	VT 280	VT 280
5	Soric SF2	E-BX 2400
6	VT 280	Stitchmat - 1.5 oz
7	CFM 0015	
8	Stitchmat - 1.5 oz	

Roof		
Layer	Gen1	Gen2
1	Stitchmat - 1.5 oz	Stitchmat - 1.5 oz
2	CFM 0015	CFM 0015
3	E-LR 1708	VT 280
4	VT 280	VT 280
5	Soric SF2	E-BX 1200
6	VT 280	CFM 0015
7	E-LR 1708	Stitchmat - 1.5 oz
8	CFM 0015	
9	Stitchmat - 1.5 oz	

Sidewall		
Layer	Gen1	Gen2
1	Stitchmat - 1.5 oz	Stitchmat - 1.5 oz
2	CFM 0015	CFM 0015
3	VT 280	VT 280
4	VT 280	VT 280
5	VT 280	E-BX 1200
6	Soric SF2	VT 280
7	VT 280	VT 280
8	VT 280	CFM 0015
9	VT280	Stitchmat - 1.5 oz
10	CFM 0015	
11	Stitchmat - 1.5 oz	

Frontwall			
Layer	Gen1	Gen1 - Center	Gen2
1	Stitchmat - 1.5 oz	Stitchmat - 1.5 oz	Stitchmat - 1.5 oz
2	CFM 0015	CFM 0015	CFM 0015
3	E-LR 2410	E-LR 2410	E-LR 2410
4	E-LR 2410	E-LR 2410	E-LR 2410
5	E-LR 2410	E-LR 2410	E-LR 2410
6	Soric SF 2	Soric XF 4	E-LR 1208
7	E-LR 2410	E-LR 2410	E-LR 2410
8	E-LR 2410	E-LR 2410	E-LR 2410
9	CFM 0015	E-LR 2410	CFM 0015
10	Stitchmat - 1.5 oz	E-LR 2410	Stitchmat - 1.5 oz
11		CFM 0015	
12		Stitchmat - 1.5 oz	

### 2.2.1 Gen1 Laminate Comparison

The ASCC conducted tensile tests and burn-off tests with Gen1 laminate coupons from each panel type in May and June of 2020. The tests followed ASTM D3039 standards and cut the composite coupons from manufactured corrugated panels. See Table A 1 row 5 for test data. The modulus of elasticity (MOE) and mass fraction (MF) were reported as ‘As Built’ properties. Using the MOE for comparison, the fabric weight in the VectorLam materials were modified until the predicted MOE matched within a reasonable percent error. Table 2 shows the iterative process.

Table 2: Gen1 Matched VectorLam MOE to As Built MOE in the 1-Direction

Panel Coupon	As Built	Attempt 0 VectorLam	% Error to As Built	Attempt 1 VectorLam	% Error to As Built	Attempt 2 VectorLam	% Error to As Built
	Msi	Msi	%	Msi	%	Msi	%
Door	2.21	2.17	2%	2.17	2%	2.17	2%
Roof	2.25	2.23	1%	2.23	1%	2.23	1%
Sidewall	3.45	3.21	7%	3.27	5%	3.32	4%
Frontwall	2.62	2.45	6%	2.48	5%	2.52	4%
Frontwall Center	2.86	2.75	4%	2.8	2%	2.84	1%

For all panels the 1-direction is parallel to the corrugations and the 2-direction is perpendicular to the corrugations. The second and third column from the left are the measured and base predicted MOE values, respectively. The fourth column shows the percent error of the predicted to the measured MOE. The predicted door, roof, and frontwall center MOE are within 5% error, an acceptable engineering prediction range, of the As Built MOE but the sidewall and frontwall MOE are not. By increasing the fabric weight of the VectorLam fabrics and recalculating the MOE for all panel coupons the predicted MOE matched the As Built MOE within 5% error. No fabric in the door and roof layups were modified due to VectorLam base fabrics predicted the MOE to be within 5%. Table 3 shows the change in fabric weight from the As Built weight to the final predict weight. Table 4 shows the change in predicted fabric weight.

Table 3: Measured to Predicted Fabric Weight Comparison

Fabric	As Built	Attempt 2 VectorLam	% Error to As Built
	oz/yd <sup>2</sup>	oz/yd <sup>2</sup>	%
Stitchmat	13.5	13.8	2%
CFM	13.7	14.0	2%
Sidewall's VT 280	28.9	30.1	4%
E-LR 2410	24.6	25.5	4%
Soric SF2	4.1	4.3	4%
Soric SF4	7.1	7.4	4%

Table 4: Initial to Final Predicted Fabric Weight Comparison

Fabric	Attempt 0 VectorLam	Attempt 2 VectorLam	% Change
	oz/yd <sup>2</sup>	oz/yd <sup>2</sup>	%
Stitchmat	13.5	13.8	2%
CFM	13.5	14.0	4%
Sidewall's VT 280	28.2	30.1	7%
E-LR 2410	23.9	25.5	7%
Soric SF2	3.5	4.3	20%
Soric SF4	7.1	7.4	4%

The As Built fabric weights were measured by using a square yard section of fabric. The fabric weights had to be increase because VectorLam tended to be conservative and under predict property values, most likely in case their results were used without coupon testing from the user.

With the MOE matching, more physical and mechanical properties were compared. Table 5 compares the weight, MOE in the 1-direction, thickness, axial stiffness in the 1-direction and the MF. Axial stiffness is calculated by multiplying the 1-direction MOE and thickness together. These properties were chosen for comparison because they are key design properties. Weight drives the cost of manufacturing and shipping. The MOE, thickness axial stiffness and MF drive the structural behavior of the container. The panels are similar to one-way bending elements due to being corrugated, thus the axial stiffness in the 1-direction the key property of the panels. This is shown in Figure 5 (20FT. Containers).



Figure 5: Primary Direction of Bending of Panels

Table 5: Gen1 Comparison of VectorLam to As Built Physical and Mechanical Properties

Panel	Weight	MOE	Thickness	Axial Stiffness	MF
	lbs	Msi	in	kip/in	%
<b>Door</b>					
As Built	37	2.21	0.292	645	46%
VectorLam	40	2.17	0.292	644	48%
% Error	8%	0%	0%	0%	3%
<b>Roof</b>					
As Built	143	2.25	0.321	722	45%
VectorLam	157	2.25	0.321	724	47%
% Error	10%	0%	0%	0%	4%
<b>Sidewall</b>					
As Built	196	3.45	0.346	1194	60%
VectorLam	195	3.32	0.346	1149	60%
% Error	1%	4%	0%	4%	0%
<b>Frontwall</b>					
As Built	108	2.62	0.356	933	47%
VectorLam	117	2.52	0.356	899	49%
% Error	8%	4%	0%	4%	4%
<b>Frontwall Center</b>					
As Built	30	2.86	0.410	1173	49%
VectorLam	32	2.84	0.410	1166	57%
% Error	8%	1%	0%	1%	17%

The weight column presents the weight for entire manufactured door, roof and sidewall panels, while it presents the non-reinforced and reinforced frontwall sections individually. The predicted panel weights are heavier, but it is expected with the extra fiber content added to VectorLam for the cause of matching the MOE which is more critical for the FEA model to properly predict structural response. The thicknesses match, thus the axial stiffness has the same acceptable percent error as the MOE because it is calculated by multiplying the MOE by the thickness. The MF matched within 5% error, except the frontwall center. Since the frontwall center layup is the same as the frontwall layup with two extra fabric layers VectorLam will predict a higher MF. However, the layups are used simultaneously in the same mold, so the measured MF will be closer than if predicted separately. Table 6 shows more physical and mechanical properties for the Gen1 door panel. The corrugations on the roof, sidewall and frontwall panels limit coupon specimens to the 1-direction, while the door panel's geometry allows for 1 and 2-direction coupon specimens to be cut. The bending rigidity is per unit width and calculated by multiplying the 2-direction MOE by the thickness cubed and dividing it by 12.

Table 6: Gen1 Door Panel Extra Physical and Mechanical Properties

<b>Panel</b>	<b>2-Direction MOE</b>	<b>Bending Rigidity</b>
	Msi	kip*in
As Built	1.02	2.12
VectorLam	1.09	2.27
% Error	7%	7%

The percent errors are 2% outside of the 5% range. The 2-direction bending rigidity is compared because it could be a driving factor for the increased yielding presented in Chapter 4 full-scale model sections.

### 2.2.2 Gen2 Laminate Comparison

The ASCC conducted tensile tests with Gen2 laminate coupons from each panel type in June and July of 2021. See Table A 1 rows 6, 7 and 8 for test data. The MOE was reported an ‘As Built’ property and compared to VectorLam Gen2 predictions similarly to Gen1. Gen2 layups used many of the same fabrics from Gen1, thus the modified fabrics from Gen1 were used from the start in VectorLam. Table 7 compares the Gen2 coupon MOE to the predicted MOE.

Table 7: Gen2 Matched VectorLam MOE to As Built MOE in the 1-Direction

Panel	As Built	Attempt 0 VectorLam	% Error to As Built
	Msi	Msi	%
<b>Door</b>	3.02	2.67	12%
<b>Roof</b>	2.55	2.63	-3%
<b>Sidewall</b>	3.29	3.24	1%
<b>Frontwall</b>	3.31	3.38	-2%

No fabric modifications were needed because most percent errors were with 5%. The door predicted MOE is not within 5% error, but the predicted axial stiffness in the 1-direction shown in is within 5% error, shown in Table 8. Table 8 also compares the weight, MOE, and thickness for each panel.

Table 8: Gen2 Comparison of VectorLam to As Built Physical and Mechanical Properties

Panel	Weight	MOE	Thickness	Axial Stiffness
	lbs	Msi	in	kip/in
<b>Door</b>				
As Built	27	3.02	0.159	481
VectorLam	30	2.67	0.181	484
% Error	13%	12%	14%	1%
<b>Roof</b>				
As Built8	104	2.55	0.210	535
VectorLam	112	2.63	0.192	506
% Error	8%	3%	9%	6%
<b>Sidewall</b>				
As Built	152	3.29	0.274	901
VectorLam	161	3.25	0.259	841
% Error	6%	1%	5%	7%
<b>Frontwall</b>				
As Built	109	3.31	0.248	820
VectorLam	120	3.38	0.259	876
% Error	10%	2%	5%	7%

The predicted panel weights have similar percent errors to Gen 1. The thicknesses are within 5% error except the door, but the key properties being axial stiffness is almost spot on for the door.

The roof, sidewall and frontwall axial stiffnesses are just outside of 5% error.

### 2.3 Generation Comparison

Table 9 compares Gen1 and Gen2 key properties such as axial stiffness in the 1-direction and 2-direction, thickness and weight.

Table 9: Comparison of Gen2 to Gen1 Predicted Key Properties

Panel	Design	Axial Stiffness in 1-Direction	Axial Stiffness in 2-Direction	Thickness, t	As Built Weight
		ksi*in	ksi*in	in	lb
Door	Gen1	643	328	0.283	37
	Gen2	303	273	0.181	27
	% Difference	-112%	-20%	-56%	-40%
Roof	Gen1	719	351	0.298	140
	Gen2	505	292	0.192	101
	% Difference	-42%	-20%	-55%	-39%
Sidewall	Gen1	1168	513	0.385	197
	Gen2	841	408	0.259	150
	% Difference	-39%	-26%	-49%	-31%
Frontwall	Gen1	891	385	0.33	134
	Gen1 - Center	1185	488	0.454	
	Gen2	841	408	0.259	109
	% Difference	-6%	6%	-27%	-23%
	% Difference Center	-41%	-20%	-75%	

The Gen1 container exceeded the ISO standards and thus the Gen2 laminate layups could be lighter and less stiff. Results will be shown in Chapter 4. Thus, the Gen2 properties are less than Gen1. Notably the door axial stiffness in the 1-direction are reduced by over half. The thickness of all panels were reduced and all panels lost substantial weight. A hybrid composite-steel container has two door panels, two roof panels, four sidewall panels and one frontwall panel. A complete set of Gen1 panels weigh 1276 lb, while a set of Gen2 panels weigh 964 lb, which is a 24% weight reduction.



## CHAPTER

### 3 FINITE ELEMENT ANALYSIS OF INDIVIDUAL PANELS

#### 3.1 Three-Point Bending Tests

Gen1 panels individually underwent a three-point bending test. The goal of this test was to verify the FEA model's ability to predict the bending behavior of each wall panel without including the complexity of the steel frame. A typical three-point bending test is where the specimen is supported by two rollers on opposite sides and away from the load, while a load is applied in the center between the supports. Both the supports and load run the full width of the specimen.

The test conducted used 2x4s for supports instead of rollers and square weights due to convenience of testing. Figure 6 shows a schematic of the conducted three-point bending test with the sidewall panel as the specimen (Snape, 2021).

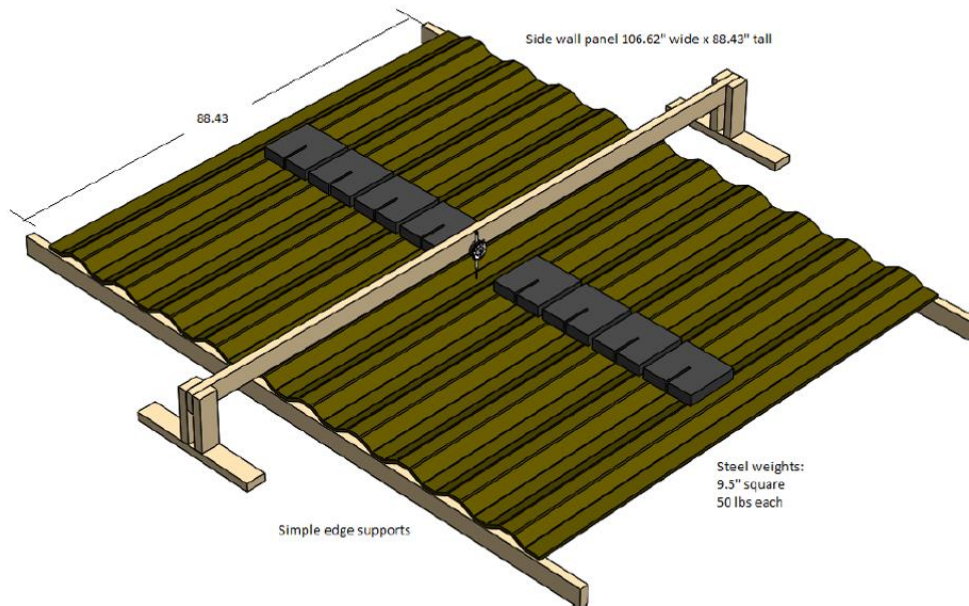


Figure 6: Three-Point Bending Test Schematic with Sidewall Panel

All the panels underwent this test to collect deflection and load data to compare to Ansys models. The test apparatus consisted of a frame made from 2x4s, 2x6s, and a metal plate to hold the dial indicator, with 2x4s used as edge supports. Nine and half inch 25 lb and 50 lb square weights were used as a load, running perpendicular and centered to the corrugations. Figure 7 through Figure 10 show the door, roof, sidewall and frontwall under load.

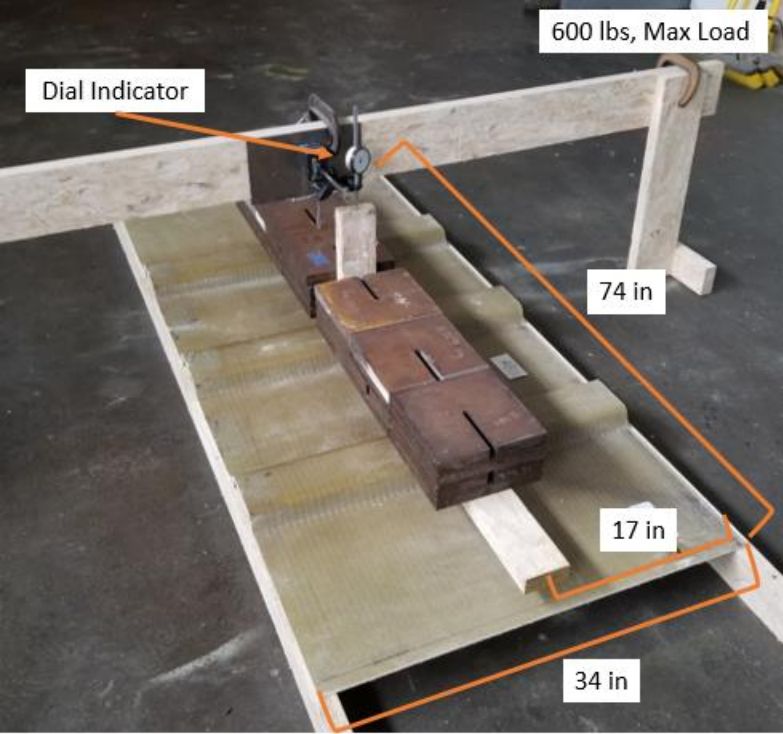


Figure 7: Door Panel Three-Point Bending Test Loaded

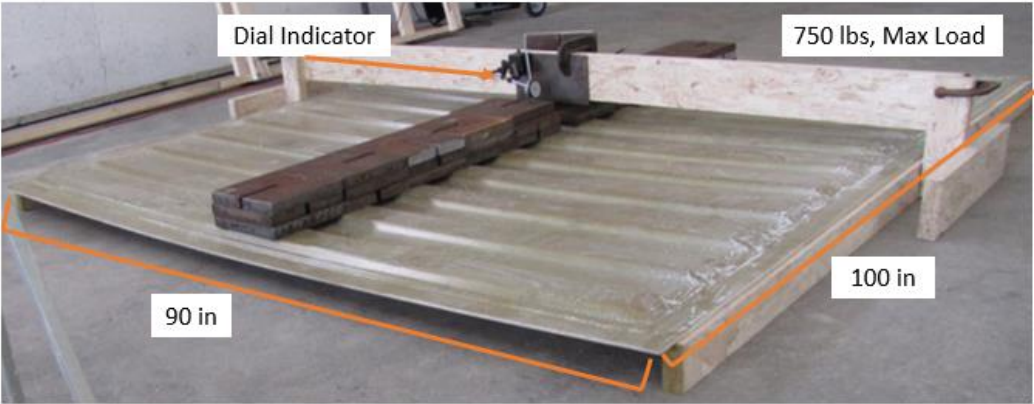


Figure 8: Roof Panel Three-Point Bending Test Loaded



Figure 9: Sidewall Panel Three-Point Bending Test Loaded



Figure 10: Frontwall Panel Three-Point Bending Test, Unloaded (Left), Loaded (Right)

Figure 7 shows the weights on a 2x4 centered on the door panel because the span between the corrugations is too large for the weights to span alone. A vertical 2x4 is on the flat 2x4 which holds the weight and is centered to middle corrugation to free the dial indicator of interference from the weights. Figure 8 shows the roof panel weights span the corrugations with no gaps for both sets of weights on each side of the dial indicator. Two 25 lb weights were placed vertically to not create a small eccentric load by interfering with the clamp hold the metal plate. Figure 9 and Figure 10 shows the sidewall panel and frontwall panel, respectively, weights centered over

the corrugation spans, thus there are gaps between each weight set. Figure 10 also shows one vertical weight, this allows the weight to not interfere with the clamp. The test results are presented in the following section and Table A 1 row 9 for the test data.

### 3.2 Ansys Three-Point Bending Test Models

The bending tests were conducted to verify that the individual panels modeled in Ansys were behaving correctly before implementing them into larger models and subassemblies. The panels are modeled as shells with eight node quadratic shell elements meshes. The material data for each layer of a panel's layup is inputted to Ansys using data from VectorLam. The layups are then compiled in Ansys and applied to the shell model. Boundary conditions (BC) and applied loads are then set. See Table A 1 row 10 for the Ansys models.

The door model BC and applied loads are shown in Figure 11.

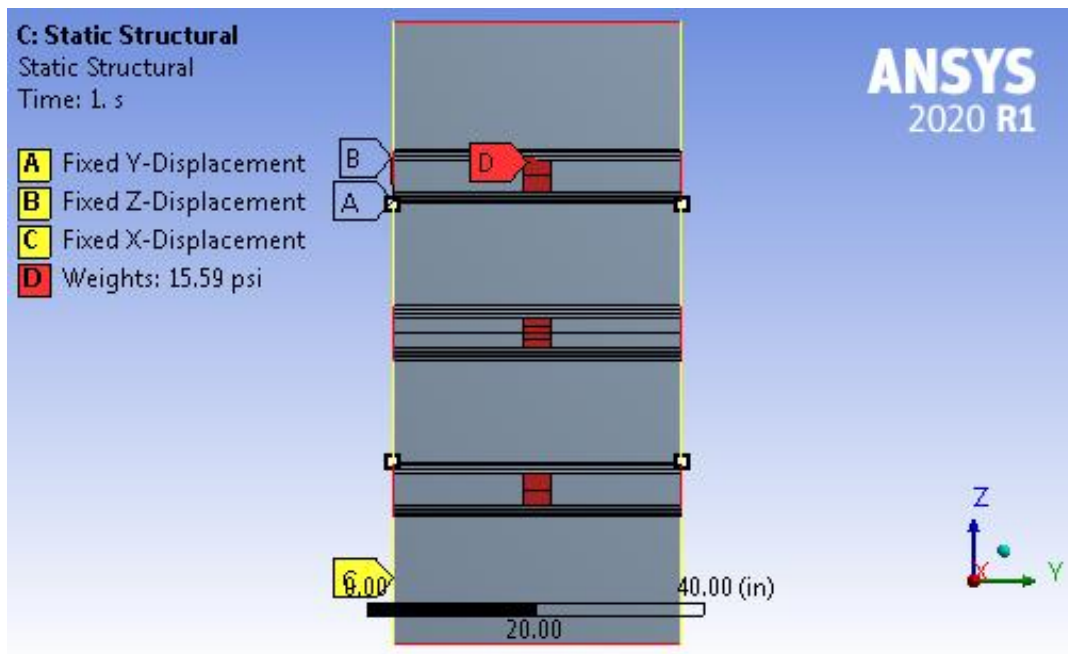


Figure 11: Door Panel, Three-Point Bending Test Ansys Setup

The yellow edges correspond to where the panel is touching the 2x4 supports. The edges are fixed in the X-direction. The BC 'B' is applied to four nodes on the panel edge, as shown above

with white squares that have a black boarder. The BC is applied to keep the model from drifting in Z-direction, to stabilize the FEA model. The BC ‘A’ is applied to the two left nodes that BC ‘B’ is applied too and fixed the nodes in the Y-direction to stabilize the FEA model. The red edges are panel edges with no BC applied because they are also free during the test. The red rectangles are where the 2x4 with the weights touch the corrugations. The load is applied as a pressure, for example the maximum weights loaded on the door panel was 600 lbs, then divided by the area of all the red rectangles, 38.48 in<sup>2</sup>, results in the 15.59 psi load shown above.

Figure 12 shows the roof models, which is set up similarly to the door model. The red edges are free, the yellow edges represent the supports and the red rectangles are where the pressure load is applied.

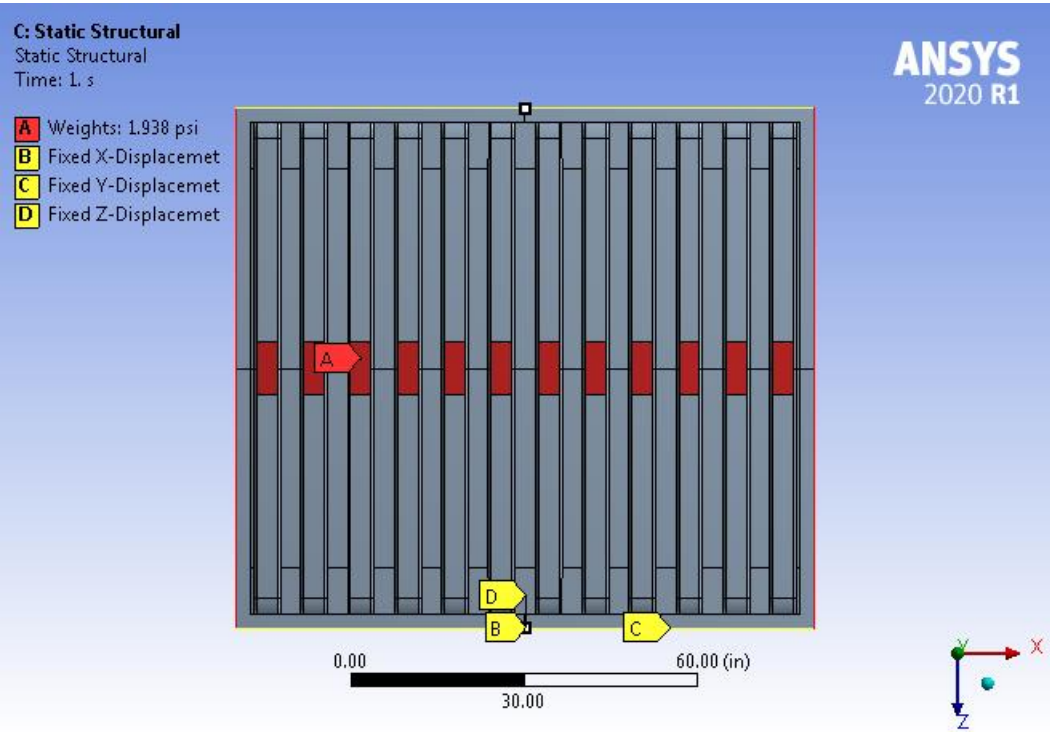


Figure 12: Roof Panel, Three-Point Bending Test Ansys Setup

The yellow edges are fixed in the Y-direction. BC 'B' and 'D' fix the same two nodes in the X-direction and Z-direction, respectively. The 1.938 psi load shown is the maximum weight loaded, 750 lbs, divided by the red rectangles area of 387 in<sup>2</sup>.

Figure 13 and Figure 14 respectively show the sidewall and frontwall models, which are set up similarly to the door and roof models. The red edges are free, the yellow edges represent the supports. However, due to gaps between the weights, it was convenient to apply the loads a line loads instead of pressures.

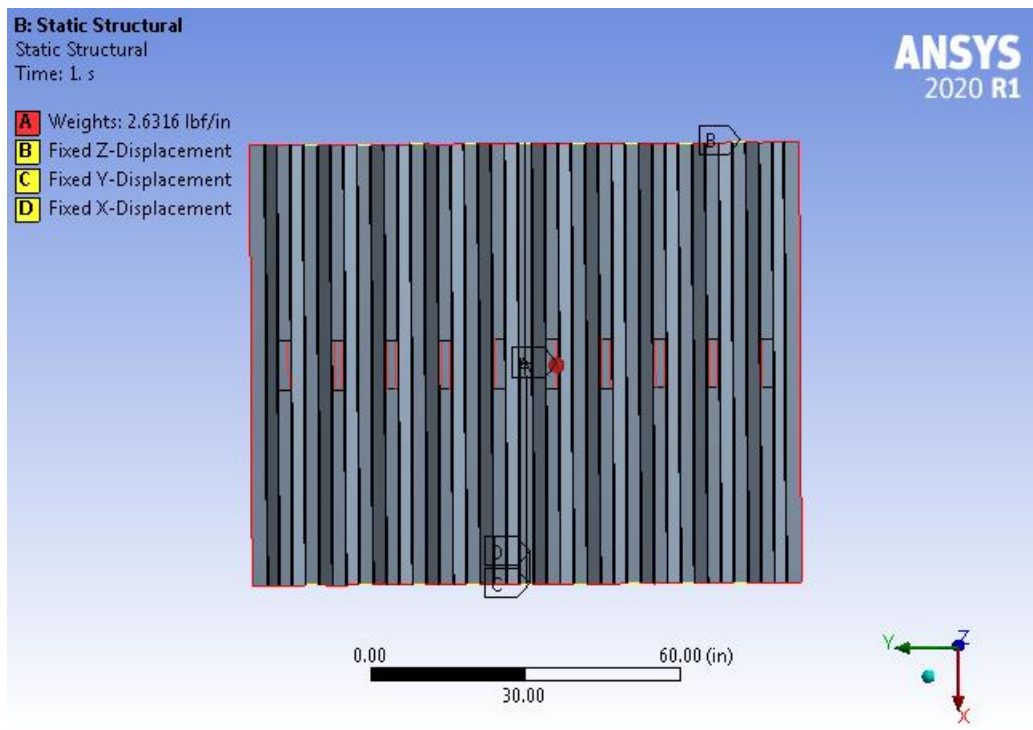


Figure 13: Sidewall Panel, Three-Point Bending Test Ansys Setup

The yellow edges are fixed in the Z-direction. BC 'C' and 'D' fix the center yellow edge on the bottom in the Y-direction and X-direction respectively. The line load was calculated by assuming the weight was a simple beam spanning the corrugation with a point load of the correct weight. The reaction forces split the weight in half to both sides of the corrugations, then it was distributed along the length of the corrugation by the width of the weights. For example, the 2.63

lb/in load shown was calculated with the maximum load of 400 lbs. Each corrugation had 50 lbs spanning it. Resulting in 25 lb reactions on each side of the corrugation, then dividing it by 9.5 in results in the load shown. The lines loads are applied where the weights edges would be touching the corrugations.

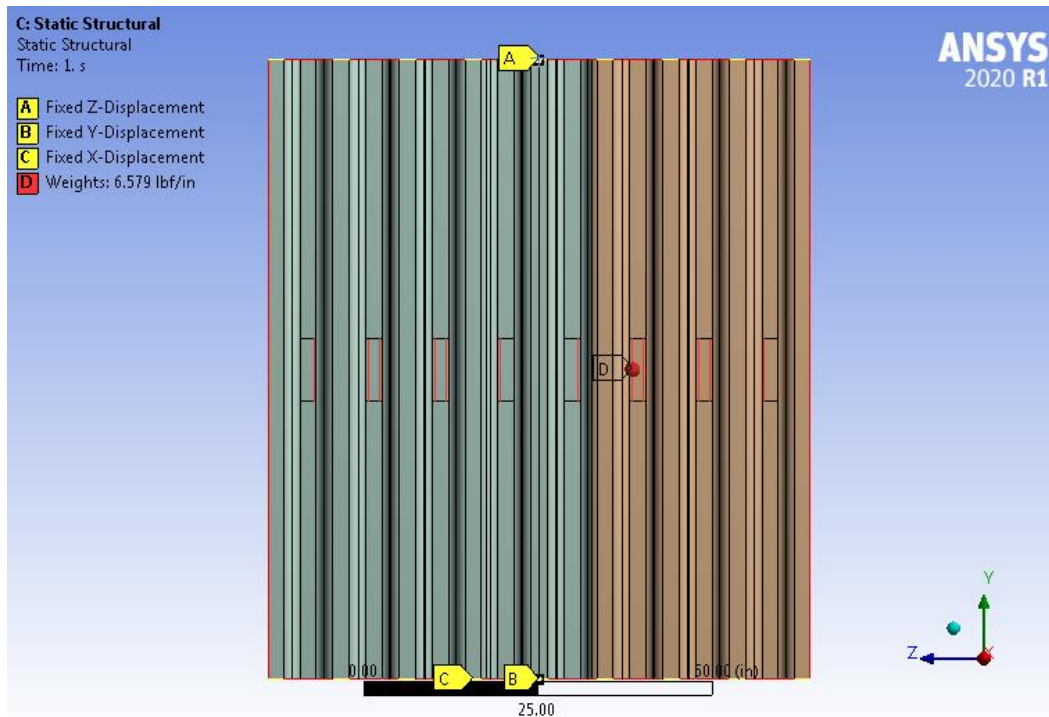


Figure 14: Frontwall Panel, Three-Point Bending Test Ansys Setup

The yellow edges are fixed in the X-direction. BC ‘A’ fixed the two center nodes on the center corrugation in the Z-direction. BC ‘B’ fixed the bottom center node of the center corrugation in the Y-direction. The line load was calculated and placement are done the same way as in the sidewall model.

The panels were modeled using small deflections and linear geometry. Choosing which nodes to stabilize the models were found by trial and error. All stabilization nodes needed to be on edges that were already used for supports. When a node on a free edge was used, the model would return stabilization errors. To keep the panels from rotating, one stabilization BC needed

at least two nodes. An edge was used in the sidewall model for stabilization because using nodes did not stabilize the model. When modeling the applied load for the door and roof models a pressure captured the test behavior well. However, in the sidewall and frontwall models line loads were used because a pressure did not capture the test behavior as accurately as possible.

Deflection data plotted from the tests and corresponding model are shown in Appendix B, as well as deflection contour plots for each panel from Ansys. In Table 10, the maximum load deflection data from the bending tests and Ansys models are compared.

Table 10: Three-Point Bending Test and Ansys Maximum Load Deflection Data

Panel	Measured Deflection	Ansys Predicted Deflection	% Error
	in	in	%
Door	0.068	0.072	5.15%
Roof	1.261	1.232	2.34%
Sidewall	0.116	0.120	3.24%
Frontwall	0.246	0.232	5.55%

The Ansys models reasonable predict the measured deflection because the percent error is below or just about above 5%. The cause of the frontwall percent error to be slightly higher than 5% could be that is a hard panel to mold and infuse due to the center reinforcement strip. Thus the thickness of the panel has a greater chance of varying throughout the panel. The behavior of the models matched reasonable to test data for container models to be developed.



## CHAPTER

### 4 FULL-SCALE CONTAINER FINITE ELEMENT MODELS

#### 4.1 Steel Verification

All the models presented in this section contain sections of the containers steel frame. Some steel sections yield during structural testing, which is critical to capture in the models to predict test outcomes. The ASTM E8 standard was used to conduct steel coupon tensile tests by the ASCC. Figure 15 shows the test set up.

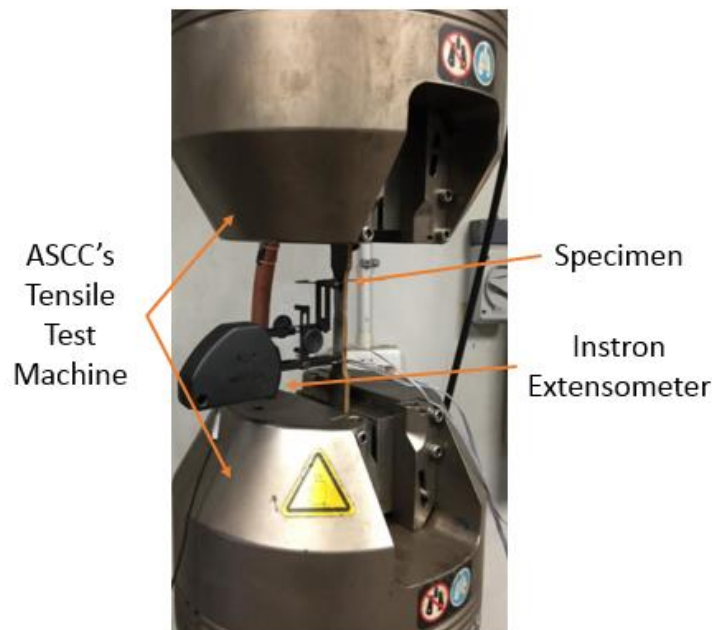


Figure 15: Steel Coupon Tensile Test Setup

Deflection was measured by an Instron extensometer. Strain could have been measured; however, a strain gauge will peel and detach from the specimen during elongation and yielding, while an extensometer will measure deflection until the specimen fails. The deflections and geometry of the specimen were used to calculate strains and stresses. The results were averaged to find the Young's modulus and create a stress-strain plot, see Figure 17. The data shown is also called the engineering stress and strain. See Table A 1 row 11 for the test data

To accurately model the material behavior in Ansys, two material models were needed. The Isotropic Elasticity material model was needed to input the Young's modulus and Poisson's ratio, thus modeling the steels elastic behavior. The Multilinear Isotropic Hardening model was chosen to model the steels inelastic behavior because it allows the plastic portion of the test data true stress-strain curve to be used as input. The geometry model of the specimen truncated the clamped sections of the specimen to match the test, which saved on elements and thus run time. It was modeled as a shell with 2325 eight node quadratic shell elements, an applied thickness and applied the corten steel material model. Figure 16 shows steel coupon model and see Table A 1 row 12 for the Ansys files.

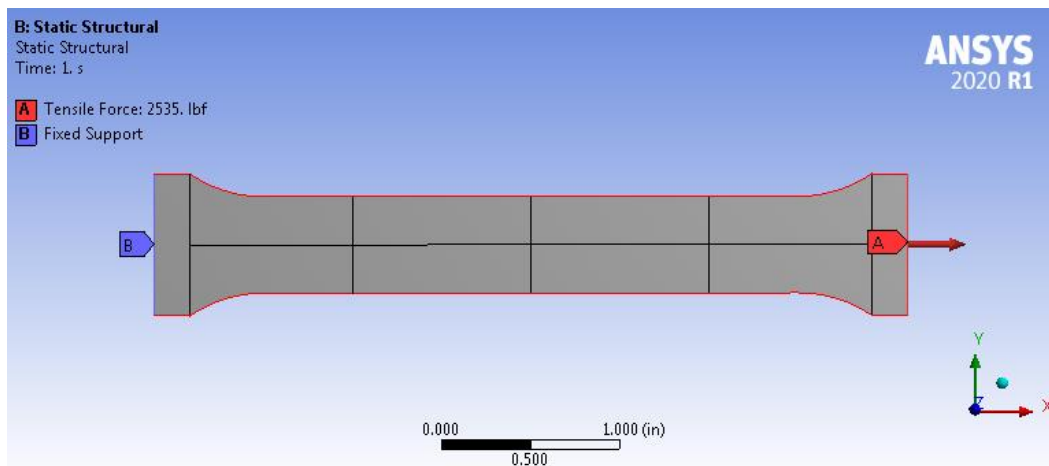


Figure 16: Steel Coupon Tensile Test Ansys Setup

The blue edge represents the clamp end during the test by being fixed in all directional and rotational degrees of freedom (DOF). The right red edge with the red arrows is edge the load is applied on, all other red edges a free. To capture the plastic deformation large deformations was turned on. Figure 17 compares the test and Ansys steel coupon engineering stress-strain curves.

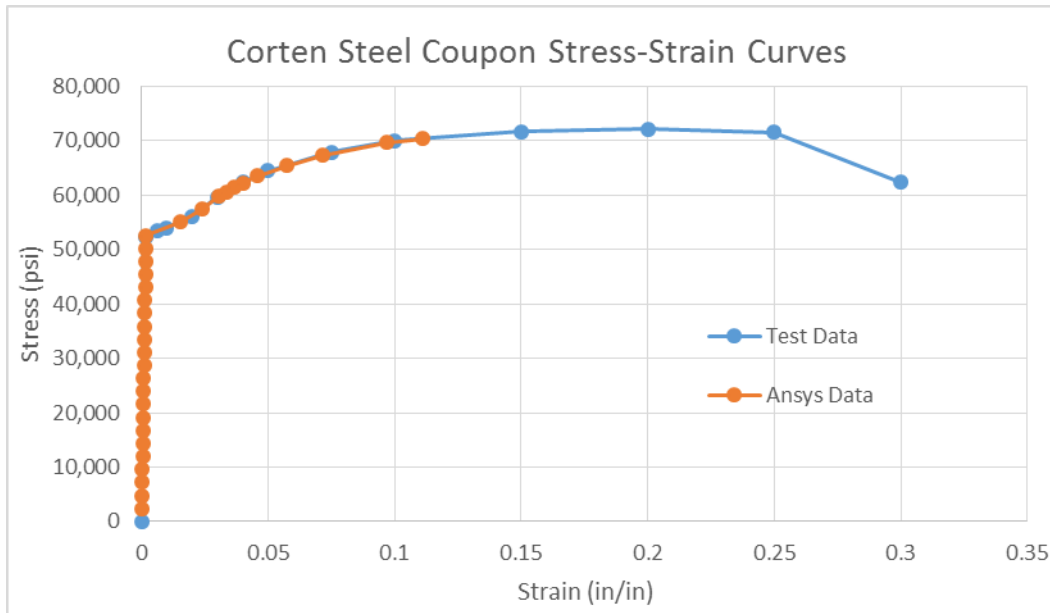


Figure 17: Comparison of Test and Ansys Steel Coupon Stress-Strain Curves

Data from the coupon model matched the test data, which verifies that the data was modeled correctly. The Ansys Data does not extend to the end of the test data because the model uses the static structural modeling tool in Ansys and not the explicit dynamic modeling tool. Thus the model returns an error when the stress limit is exceeded. This allows the model to run faster and is appropriate to use because no steel component was stressed to the point of failure during the ISO testing.

#### 4.2 Sidewall Strength Test

The sidewall strength test was determined to be a key structural response due to prior University of Maine Testing, which showed the steel tab yielding during tests, thus making the container fail ISO dimensional requirements. Summarizing from ISO 1496-1 sidewall strength test section, the container must prove its ability to withstand forces resulting from ship movements. The entire sidewall must be subject to a uniformly distributed internal load of 0.6 P. Both sidewalls must be tested if the container is asymmetric and the test must not restrain the

sidewall and its longitudinal members from deformation. From ISO 1496-1 Annex A, Figure 18 presents a schematic of the loading.



Figure 18: ISO 1496 Annex A Figure A.8.

The load shown within the container represent uniformly distributed internal loads and are for the whole container. After the test, the container cannot have permanent deformations or abnormalities which render its unsuitable for use. Thus the sidewall must not protrude past a plane created by the corner castings, which is required to not interfere with other containers beside it. The sidewall must also not permanently deflection more than 0.32 in per ISO/TR 15070. The test setup is shown in Figure 19.

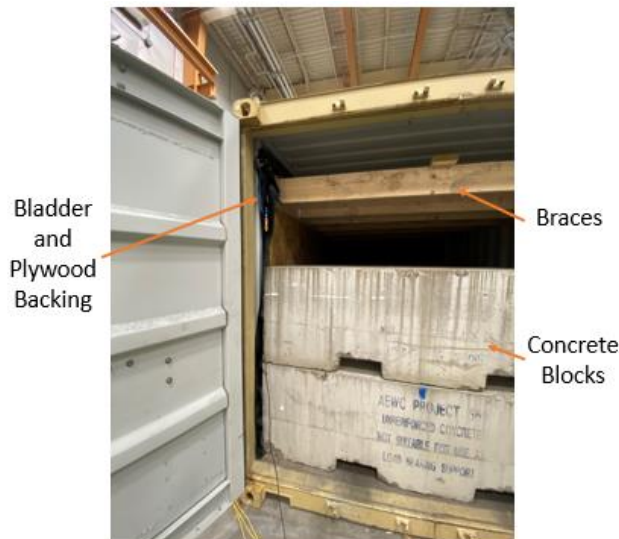


Figure 19: Sidewall Strength Test Setup

The bladder and plywood are put in place first, then the concrete blocks and braces above them are put in simultaneously. The blocks and braces are used to keep the bladder fully against the wall. The bladder is slowly pumped up to 2.6 psi to uniformly distribute the 0.6 P load required. Then the bladder pressure is released and finally the blocks are removed. The dimensional

checks are made after the container is empty. Figure 20 shows the container loaded. Figure 21 and Figure 22 show where string pots and strain gauges are located on the container, respectively. These strain gauge locations will also be used for the fork-lift pocket lifting test. See Table A 1 rows 13 for test data.



Figure 20: Sidewall Strength Test Loaded

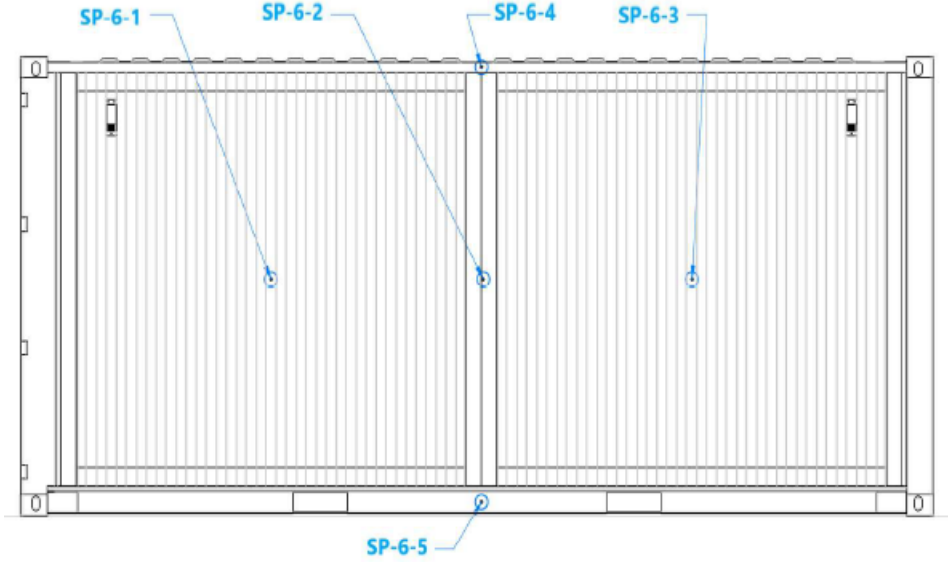


Figure 21: String Pot Locations on the Sidewall

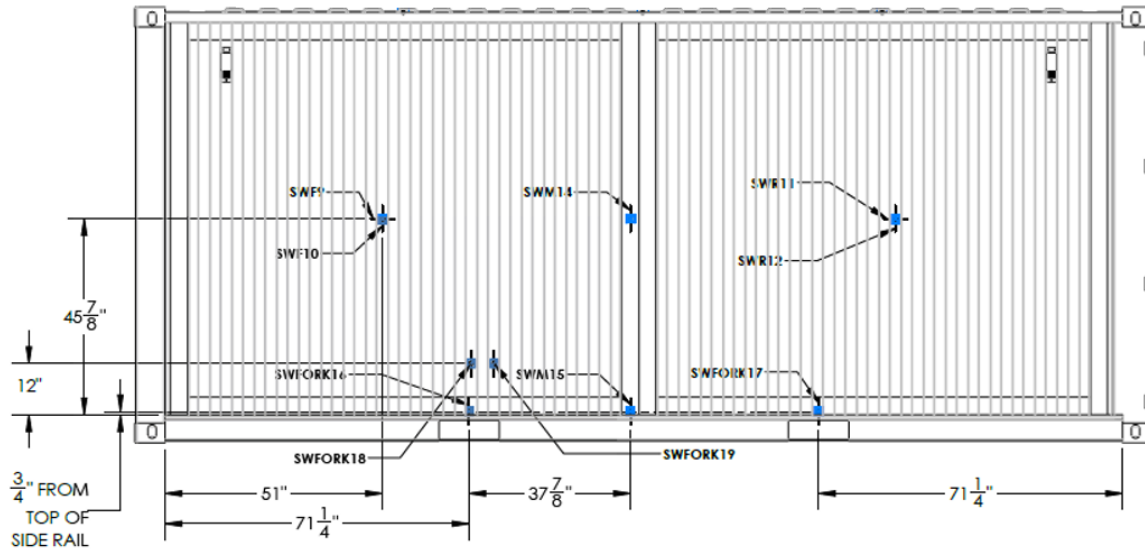


Figure 22: Strain Gauge Locations on the Sidewall

#### 4.2.1 Development of Ansys Sidewall Strength Test Model

To model the sidewall strength test, it was determined that at least half of the container needed to be modeled to capture the containers behavior correctly. A half model of the container included: the sidewall panels, steel tabs connecting the panels to the steel frame, top side rail, bottom side rail, corner posts, half the roof and half the floor. Throughout the modeling process of the test, three model versions were created and each version modified the previous. The geometric modeling process for Version 1 took place in Ansys's geometry program Space Claim and began with the geometric section of the three-point bending test sidewall model. The sidewall panel edges were increased to accommodate the overhanging steel tab and its faces sectioned to distinguish the composite panel and steel tab, then it was duplicated and arranged side by side. The corner posts, top side rail and bottom side rail were then modeled and arranged into their positions. A flat plate to represent half the roof panel and the cross members with half their lengths were modeled and arranged into their positions. The new components were shell models like the sidewall panel.

The model was meshed with 236,503 eight node quadratic shell elements. The material data sidewall and roof panel layups were inputted to Ansys using data from VectorLam. The layups were then compiled in Ansys and applied to their sections of the shell model. The corten steel material model was then applied to all the remaining locations, along with the appropriate thickness. BC and applied loads are then set. Figure 23 shows the BC for the Version 1 model.

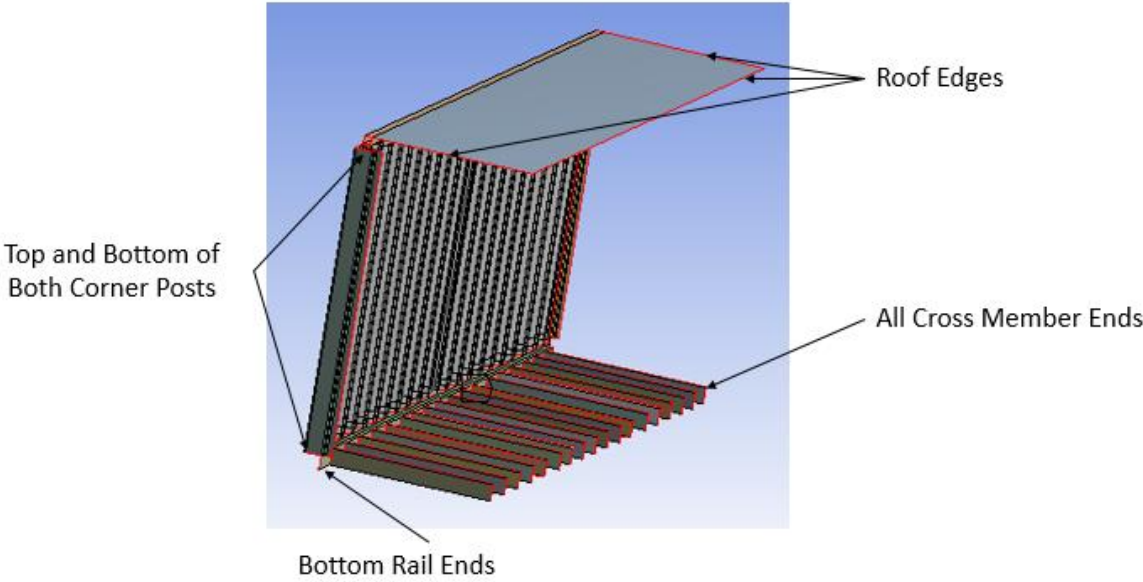


Figure 23: Sidewall Strength Test Version 1 Model Boundary Conditions

All called outs are to edges that are fixed from displacements and rotations. Figure 24 shows the deflection results of a unit pressure applied to the inside of the sidewall, both panels and the steel tabs.

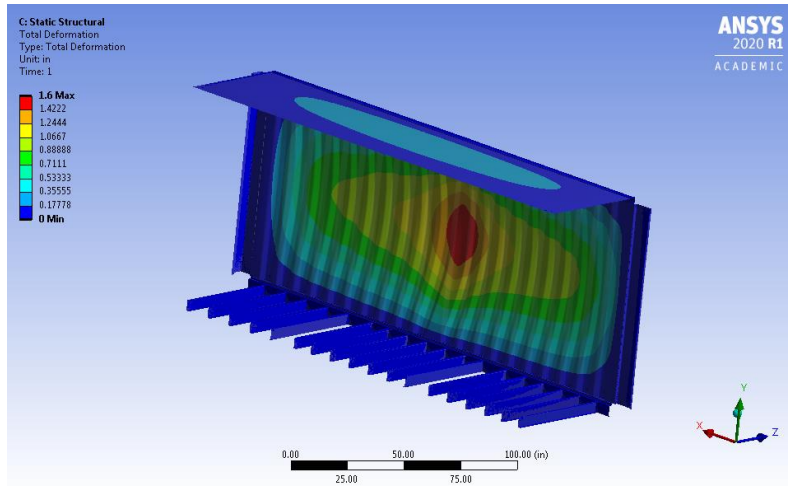


Figure 24: Sidewall Strength Test Version 1 with Unit Pressure Applied

The results shows that the model captures the general behavior of the sidewall. This model is only half of a container, which limits the number of elements and results in shorter run times. To more accurately represent the roof, full roof panels and steel tabs could be inserted into the model. To accurately model the concrete block load the cross members need to be covered by the floor. These limitations led to the second version of the model.

Version 2 now includes the roof panel with steel tabs and the container floor covering the existing cross members. Figure 25 shows Version 2.

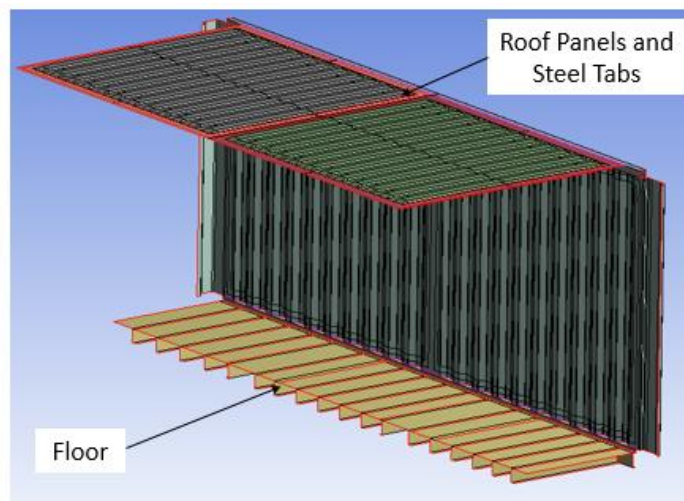


Figure 25: Sidewall Strength Test Version 2



The steel tabs for the roof panel were model by increasing the panel edges and sectioning the tabs and panel off. The floor was necessary to apply the concrete block pressure load accurately to and to stiffen the cross members.

The mesh consists of 241,581 elements, 2.1% more elements than Version 1. The BC from remain along with the addition of the floor edges being fixed too. Version 1 only had the wall pressure load, but too accurately simulate the test the loading is broken down in to four steps. First the concrete blocks load was applied as a pressure to the floor, then the wall pressure is applied as in Version 1. Then the wall pressure is released. Finally the concrete block pressure is released.

This version more accurately models the roof and flooring system, but the boundary conditions do not accurately reflect a symmetrical system. Figure 26 shows the model under only a unit concrete block pressure applied to the floor.

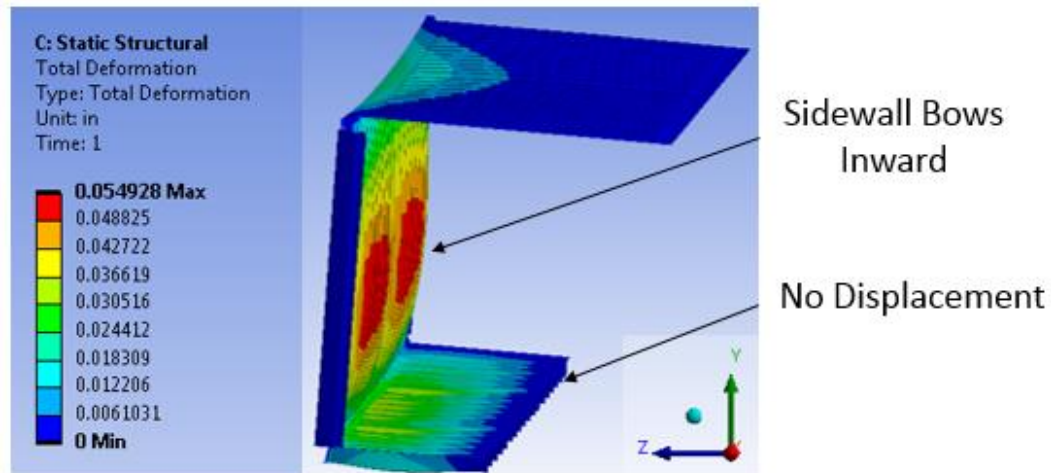


Figure 26: Sidewall Strength Test Version 2 Concrete Block Load

The sidewall bows inward as seen during the test, however the center of the floor does not move. This is due to floor and cross member central edges being fixed in space which does not

represent the actual system. This model more accurately models the roof, but the BC do not capture the containers behavior, thus this limitation led to Version 3.

Version 3 is a mirrored structural system of Version 2 around the end of the floor and cross members, without the roof being duplicated. Figure 27 shows Version 3 and its BC and loads.

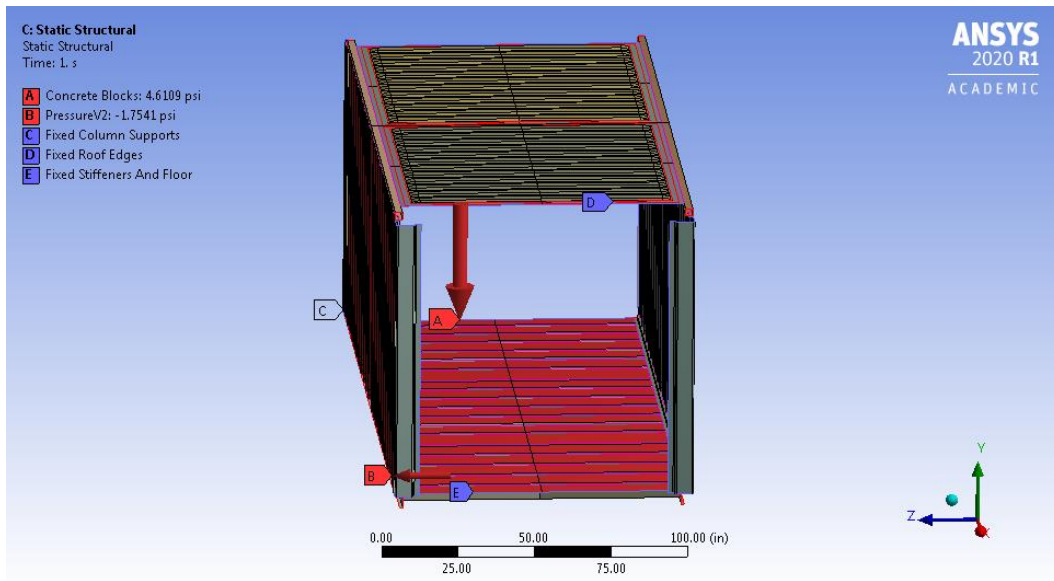


Figure 27: Sidewall Strength Test Version 3

The mesh consists of 469,410 elements, 49% more elements than Version 2. The corner posts and roof BC remain unchanged, while the only the floor edges that would connect to the door and frontwall are fixed. Figure 28 shows Version 3 with only the concrete block load applied.

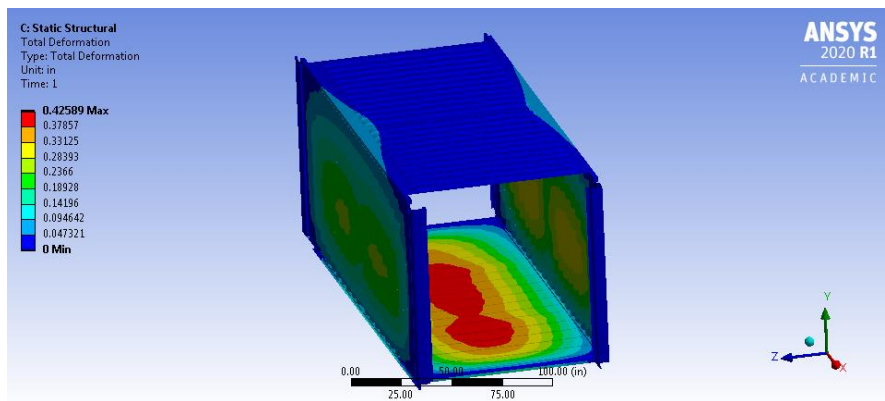


Figure 28: Version 3 Deflection Contour Plot for Concrete Block Load

With the maximum deflection in the center of the floor and dispersing outwards, Version 3 captures the concrete block load behavior correctly. Moving forward non-linear geometry and non-linear material models will be turned on. Version 3 now captures the general behavior of the test and for the remainder of this paper Version 3 will be referred to as the sidewall model. See Table A 1 row 14 for the Ansys files.

### 4.2.2 Comparison of Full-Scale Test Data to Ansys Data

A Gen1 container underwent the sidewall strength test and the maximum deflection recorded was 3.86 in. The sidewall model predicted a deflection of 4.09 in, a 5.1% error. With the model maximum deflection results near the test data, a mesh convergence study was conducted to verify that the FEA model converged on a solution. Figure 29 shows a graph of the study. See Table A 1 rows 15 for graph data.

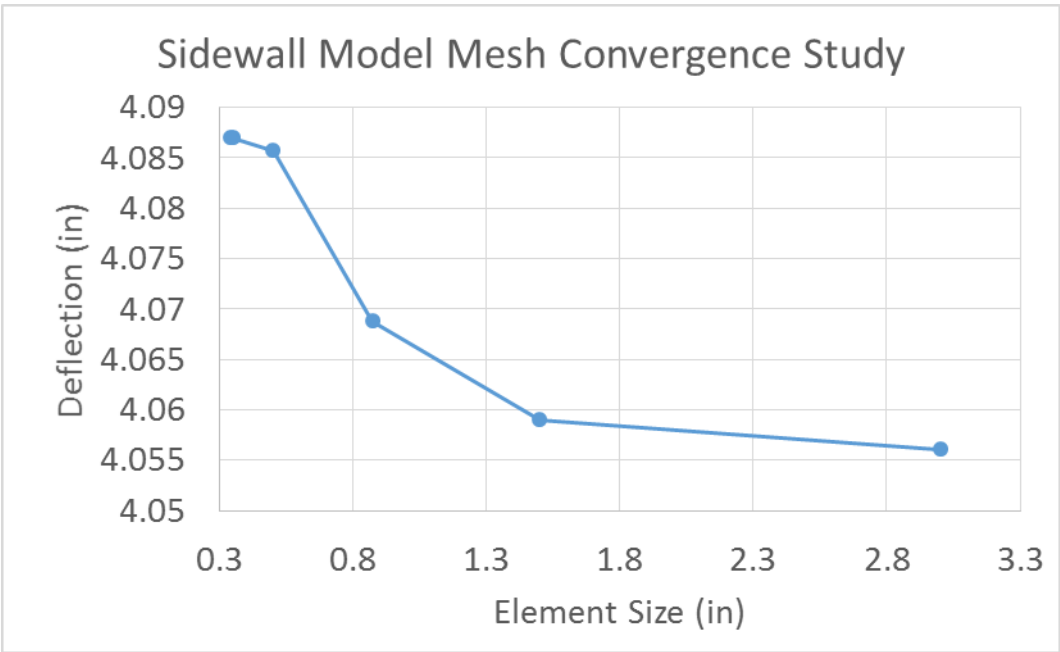


Figure 29: Sidewall Model Mesh Convergence Study

The deflection shown is the sidewall mid-span deflection with the bladder fully loaded. Ansys set the default mesh size to 0.85 in, with 469,410 elements. The mesh size was increased up to

three inches and reduced to 0.34 in. This range gave deflection results with meshes that have just over 250,000 to 1,061,859 elements. The deflection appeared to be converging with a mesh size of 0.34 in, which took over 10 hours per simulation and with limitations due to computer memory this is the mesh size used in all future simulations.

Table 11 compares the mid-span deflections under the full test load and the residual deflection for Gen1 and Gen2 containers and models. See Table A 1 rows 15 for comparison data.

Table 11: Comparison of Sidewall Strength Test Mid-Span Deflection

Container	Full Test Load	Residual
	in	in
Gen1 Test Data	3.86	0.09
Ansys Model	4.09	0.13
Percent Error	5.5%	27.3%
Gen2 Test Data	4.84	0.10
Ansys Model	5.06	0.35
Percent Error	4.2%	71.1%

Both generation containers measured data satisfy the test residual requirements of no more residual deflection than 0.32 in. The Gen1 container resulted in a 5.5% error while under the full test load, this is just outside of the acceptable engineering prediction range of 5%. While the residual deflection had a 27.3% error, but only off by 0.04 in and satisfies the test residual requirements. The Gen2 container was with the acceptable range with 4.2% error during the full test load. However, the Ansys residual deflection is significantly different from the tests and does not satisfy the test residual requirements. Figure 30 shows the Gen2 test and Ansys load versus pressure data plotted for the mid-span deflection. See Table A 1 row 16 for graph data.

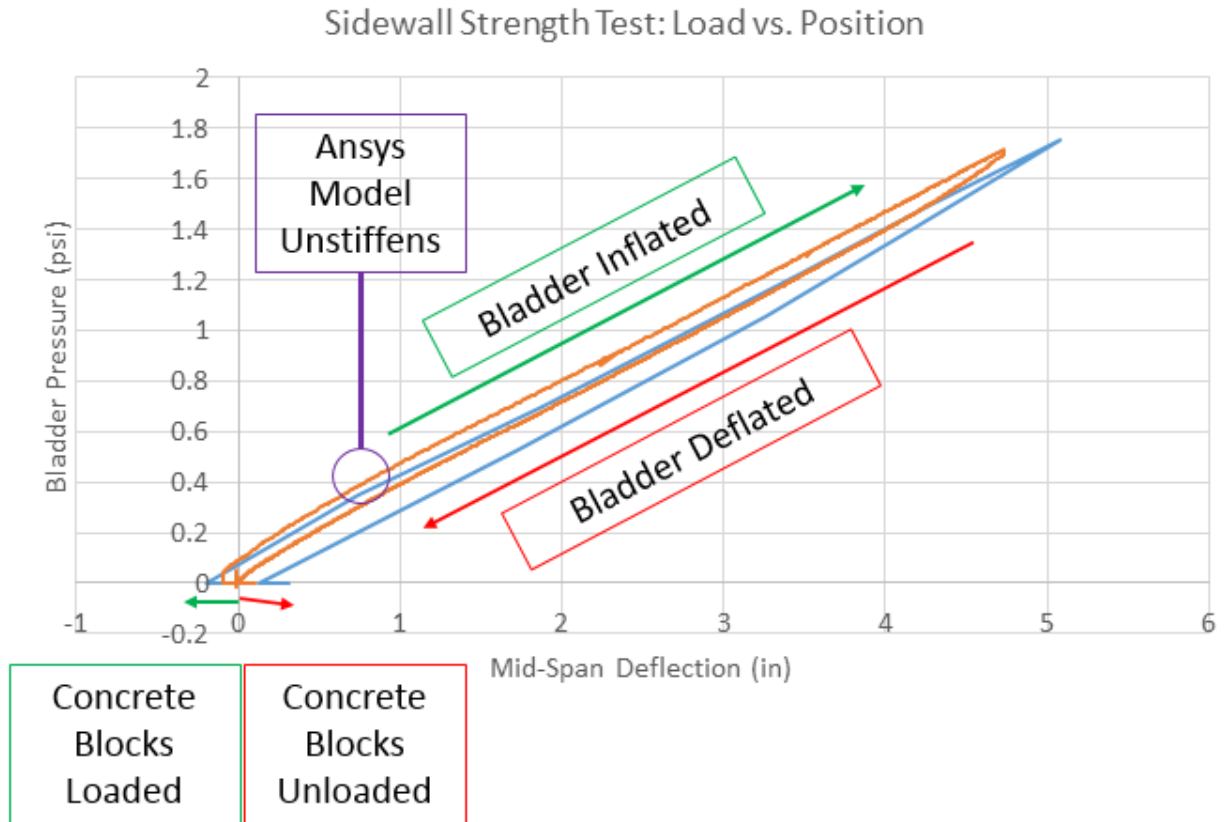


Figure 30: Sidewall Strength Test: Load vs Position Graph, at Mid-Span

The graph illustrates the Ansys model losing stiffness, thus deflecting and yielding more. It shows that the model captures the test behavior while being loaded, but not while being unloaded. This could be due to the model's geometric limitations, such as; not modeling the door sill, door system, front sill and frontwall.

Table 12 compares the strain data between the test and model for Gen1 and Gen2 containers for relevant strain gauges. These strain gauges were chosen because they cover the full bending of both sidewall panels and steel tabs, while the gauges on the lower half of the sidewall are for the fork-lift pocket lifting test. Refer to Figure 22 for strain gauge locations. The strain gauges 9, 11 and 14 are oriented vertically to capture the global bending, while gauges 10 and 12 are oriented horizontally to capture the local bending aspects. Positive strains indicate tension and negative strains indicate compression.

Table 12: Comparison of Sidewall Full Test Load Strains

Container	Strain Gauge ( $\mu\epsilon$ )				
	9	10	11	12	14
Gen1 Test Data	-1208	2783	N/A	N/A	-118
Ansys Model	-1062	2904	-1059	2905	-200
Percent Error	13.7%	4.2%	N/A	N/A	41.0%
Gen2 Test Data	-1596	3398	-1343	3346	N/A
Ansys Model	-1636	3524	-1636	3522	-258
Percent Error	2.4%	3.6%	17.9%	5.0%	N/A

The measured and predicted strains verify the model captures the test behavior, however the sidewall model over predicts the strains. Only gauge 10 in Gen1 was under acceptable percent error, but gauge 9 was close to the acceptable range. Gauge 14 is not close to the acceptable range, but predicts the correct sign and is close in magnitude. Gauge 10's location makes it difficult to predict because it is in between the weld connecting two sidewall panels and the adhesive bond connecting the steel tab and sidewall panel. Gen2 gauge 11 was the only Gen2 gauge outside the acceptable range. This is most likely due to slight variations during the full-scale testing because the model predicts the same result for the both sidewall panels.

#### 4.2.2.1 Modeling Techniques

The development of the sidewall model included many techniques that will be carried out the models presented in later sections of this chapter. The non-linear geometry and non-linear material model for the steel were key to capture residual effects from the test on the container. Querying deflection and strains from the model began with used just the max and min tools provide by Ansys or sectioning off a face of the model to create a node at the desired location. In the result section of Ansys, free local coordinate system could be placed anywhere on the model. The coordinate system could then be used to query information, the model did not have to be meshed and run again like it would after creating a new node location.

Since the sidewall bows inward with the concrete load, the floors thickness and material properties were modified to see its effect on the results. No signification change occurred, so the floor properties were restored to their original values. The geometry of sidewall panels, corner posts and bottom side rail were simplified. No ventilation holes were modeled in the panels and no lashing bars were modeled in the corner posts. The fork pocket holes were not cut out of the bottom side rail component.

#### **4.2.3 Model Conclusions**

The sidewall model accurately captures the concrete block load and the sidewall full test load behavior. Under the concrete load, the floor and cross members deflect towards the center of the container and the sidewalls bow inward. The full test load represents the global bending of the sidewall and the Gen2 test data is over predicted by 4.4% error. The residual deflection over predicts the Gen2 test data with a 71.1% error. The strains are predicted within an 11% error for Gen2, except for gauge 14.

#### **4.3 Roof Strength Test**

The roof strength test was determined to be a key structural response because it was unknown if the steel tab would yield during ISO testing. Summarizing from ISO 1496-1 roof strength test section, the container must prove its ability to withstand forces resulting from people walking on it. The roof must be subjected to a uniformly distributed internal load of 300 kg over an area of 23.6 in x 11.8 in on the weakest area of the roof. From ISO 1496-1 Annex A, Figure 31 presents a schematic of the loading.

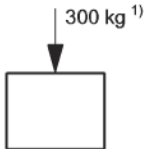
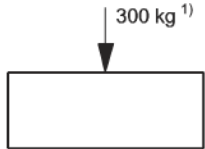
	Roof load Test No. 7	
A.9		
	Applicable where a rigid roof is provided	Applicable where a rigid roof is provided

Figure 31: ISO 1496-1 Annex A Figure A.9

The loads shown are externally applied. After the test, the container cannot have permanent deformations or abnormalities which render its unsuitable for use. Per ISO/TR 15070 the roof cannot permanently deflect more than 0.16 in. The test setup is shown in Figure 32.

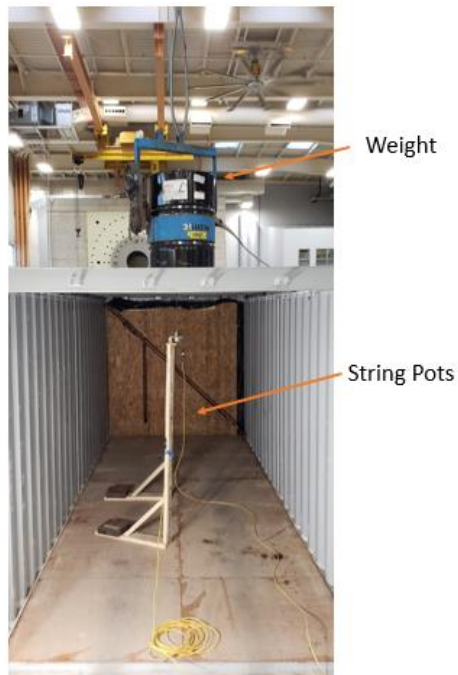


Figure 32: Roof Strength Test Setup

Since the weakest area of the roof is unknown, two locations were tested individually. One in the center of the roof and the other in the center of the roof panel, as shown by the string pots. Figure 33 shows that at each location the weight was orientated in two directions to determine the weakest position.



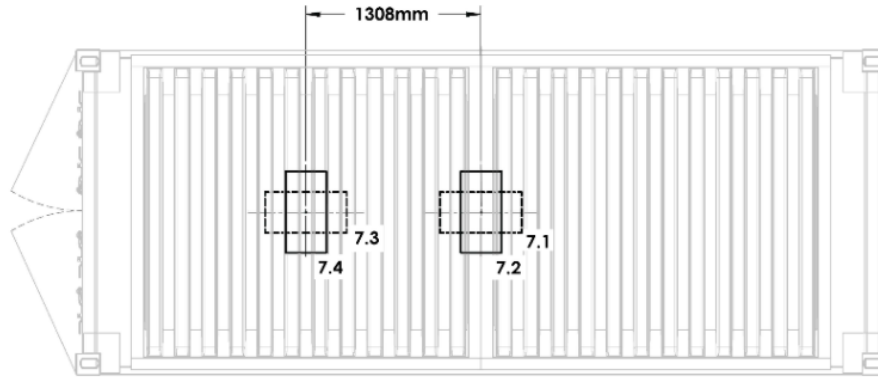


Figure 33: Roof Strength Test Load Positions

From testing it was determined that position 7.4 was the weakest due the largest deflection occurred there. See Table A 1 row 17 for the test data. The four positions are labeled as 7.1 through 7.4 because the roof strength test is marked as the seventh test from ISO 1496-1

#### 4.3.1 Development of Ansys Roof Strength Test Model

Since the sidewall model created for the sidewall strength test includes an accurate roof component, the model was modified for the roof strength test. The BC remained the same. The roof panel was sectioned to form the area for position 7.4. Figure 34 shows the roof strength test BC and load setup. See Table A 1 row 18 for the Ansys files.

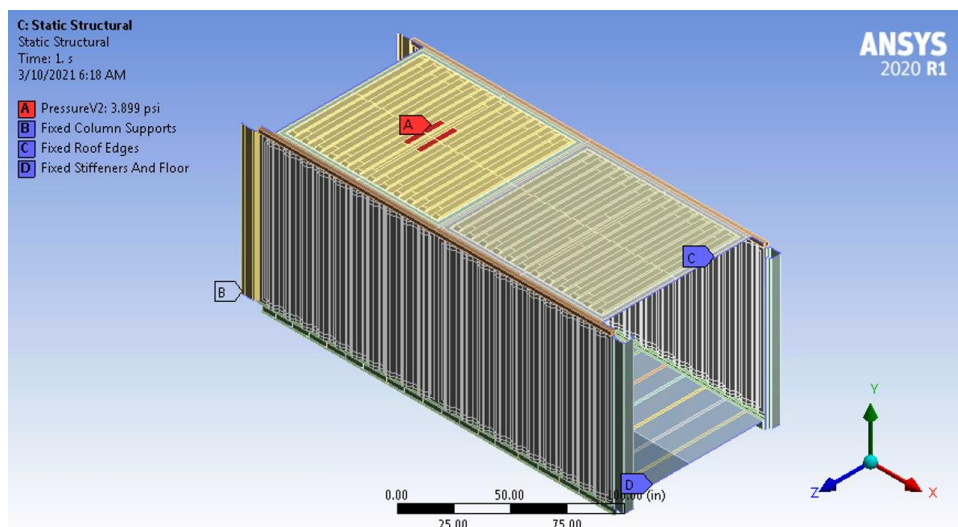


Figure 34: Roof Strength Test BC and Load

The concrete block load and wall pressure load were deleted, to be replaced with a pressure load on top of the roof panel in position 7.4.

**4.3.2 Comparison of Full-Scale Test Data to Ansys Data**

Both generation containers passed the roof strength test. The roof model over predicted the full test load deflections but matched the residual deflections well. Table 13 compares position 7.4 center deflections under the full test load and the residual deflection for Gen1 and Gen2 containers and models. See Table A 1 row 19 for the comparison data.

Table 13: Comparison of Roof Strength Test Position 7.4 Center Deflection

Container	Full Test Load	Residual
	in	in
Gen1 Test Data	1.49	0.010
Ansys Model	1.59	0
Percent Error	6.2%	-
Gen2 Test Data	1.81	0.004
Ansys Model	2.24	0
Percent Error	19.3%	-

The model over predicts the Gen1 full test load deflection by 6.2% error and by 19.3% error for Gen2. Percent error cannot be calculated for the residual deflection for both generations because the model did not predict any. The deflection measured is small enough to be slight movements in the string pots connection to the roof panel. Thus, the panels did not deform, which matched the models.

**4.3.3 Modeling Conclusions**

By including a detailed roof component in the sidewall model, the roof strength test model used the same geometry and BC. Saving time creating and verifying another model. Unlike the sidewall model, the roof model did not predicted the full test load deflection accurately, shown

by the 19.3% error for Gen2. However, the roof model still passed the roof strength test because there residual deformations match, being close to 0 in for the test and 0 in for the model.

#### 4.4 Frontwall Strength Test

The frontwall strength test was determined to be a key structural response because it was unknown if the steel tab would yield during ISO testing. Summarizing from ISO 1496-1 the frontwall strength test section, the container must prove its ability to withstand external longitudinal restraint under the dynamic conditions of operations on a railway. The frontwall must be subject to a uniformly distributed internal load of  $0.4 P$ , while allowing the frontwall to deflect freely. From ISO 1496-1 Annex A, Figure 35 Figure 31 presents a schematic of the loading.

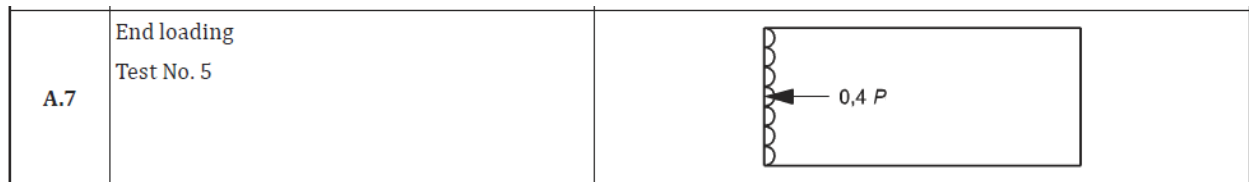


Figure 35: ISO 1496-1 Annex A Figure A.7

The loads shown within the container represent uniformly distributed internal loads and are for the whole container. After the test, the container cannot have permanent deformations or abnormalities which render its unsuitable for use. Thus the frontwall must not protrude past a plane created by the corner castings. Per ISO/TR 15070 the frontwall cannot permanently deflect more than 0.28 in. The test setup is shown in Figure 36 and Table A 1 row 20 shows the test data.



Figure 36: Frontwall Strength Test Setup

The bladder and plywood are put in place first, then the concrete blocks. The blocks are used to keep the bladder fully against the wall. The bladder is slowly inflated to uniformly distribute the 0.4 P load required. Then the bladder pressure is released and finally the blocks are removed. The dimensional checks are made after the container is empty. Figure 37 shows the container loaded. Figure 38 shows where strain gauges are located on the frontwall.



Figure 37: Frontwall Strength Test Loaded

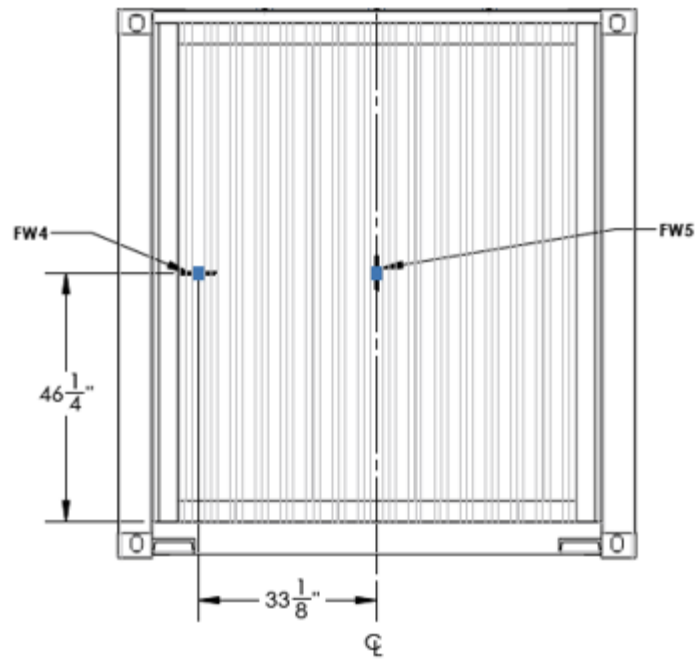


Figure 38: Strain Gauge Locations on the Frontwall

#### 4.4.1 Development of Ansys Frontwall Strength Test Model

In this section and the remaining sections of this thesis, the frontwall strength test model, will be called the frontwall model which was developed with the same process as the sidewall model.

The frontwall panel geometry, from the three-point bending test model, edge lengths were increased and sectioned off for the overhanging steel tab. The corner posts, top front rail, front header and front sill were modeled and arranged into their positions. The model has an element size of 0.87 and 164,493 eight node quadratic shell elements. The frontwall layups and steel material models were inputted into Ansys and applied to the shell model using the same process as done in the sidewall model. The applied load and initial BC are then set and shown in Figure 39.

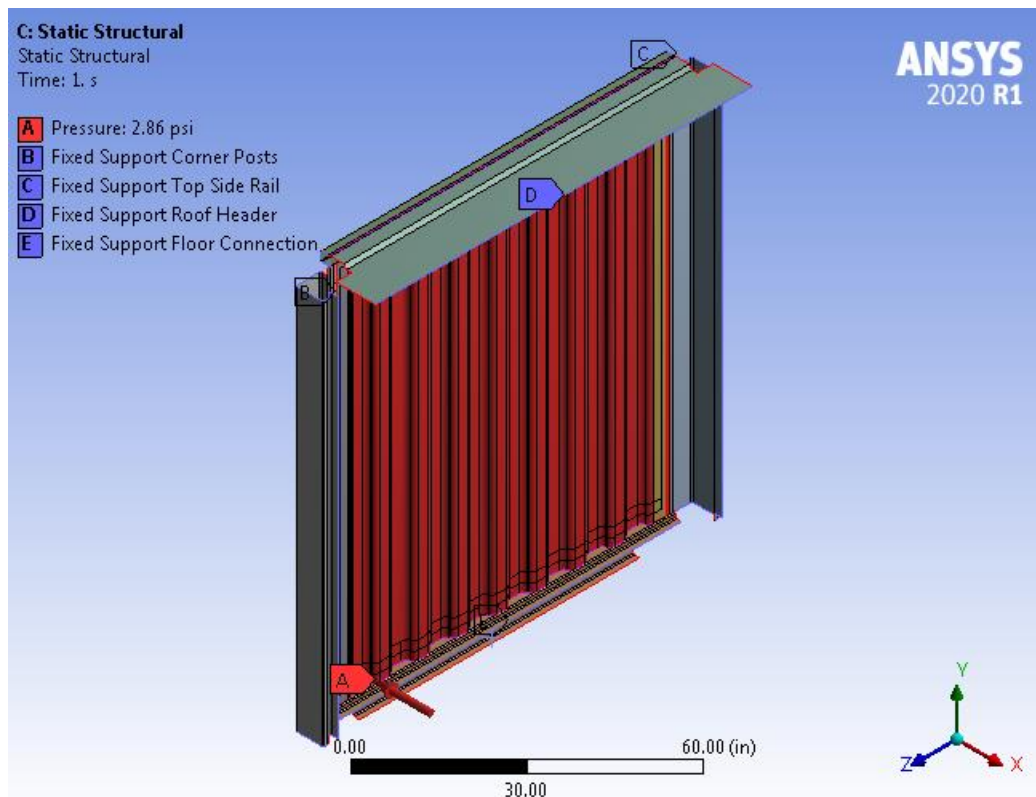


Figure 39: Frontwall Model Load and Initial BC

The exposed edges of the top front rail and corner posts are fixed from displacements and rotations. The top edge of the front sill which would be attached to the floor and edge of the front header which would be connected to the roof are also fixed.

#### 4.4.2 Comparison of Full-Scale Test Data to Ansys Data

A Gen1 container underwent the frontwall strength test and the maximum mid-span deflection recorded was 3.06 in. The frontwall model predicted a deflection of 2.95 in, a 3.9% error. However, the measured and predicted residual deflection were 0.22 in and 0.54 in, respectively. Thus the frontwall model had a 59.6% error when predicting the residual deflection. Modifications to the BC were made to capture the residual deflection more accurately and are shown in Figure 40. See Table A 1 row 21 for the Ansys files.

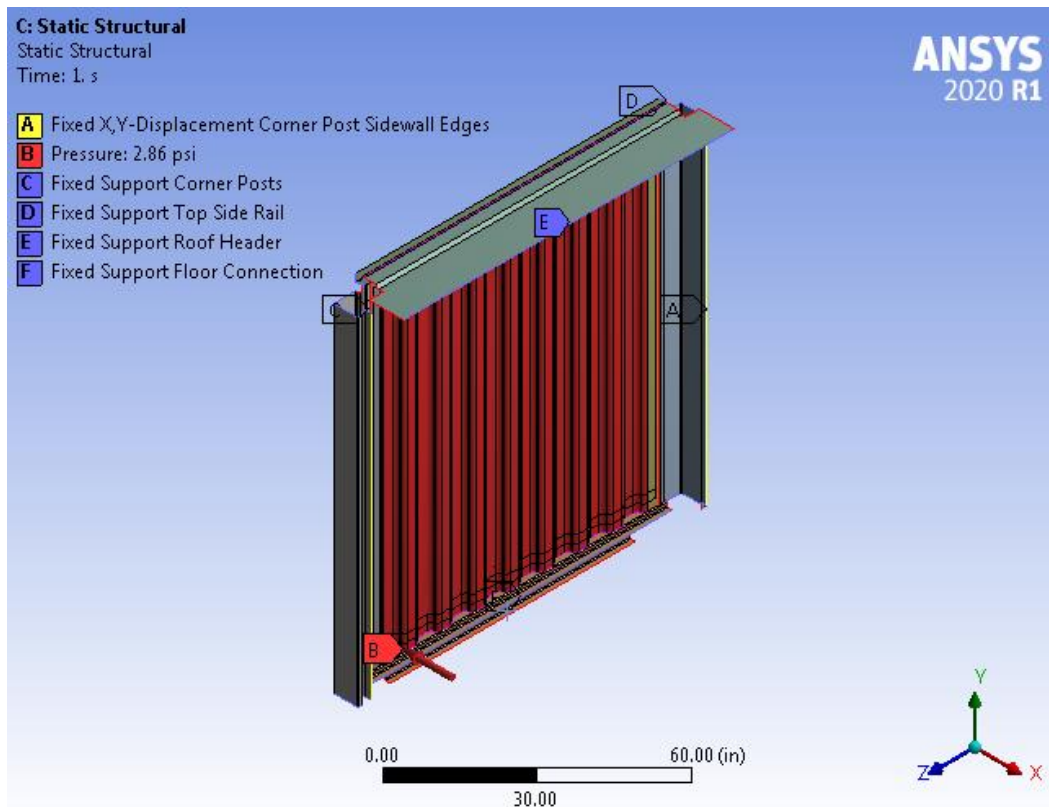


Figure 40: Frontwall Model Load and BC

The BC on the front top rail, sill and head remained the same. The corner posts vertical edge which would connect to the sidewall only restriction is the X and Y-displacements are fixed.

Table 14 compares the mid-span deflections under the full test load and the residual deflection for Gen1 and Gen2 containers and models with the updated BC. See Table A 1 row 22 for comparison data.

Table 14: Comparison of Frontwall Strength Test Mid-Span Deflection

Container	Full Test Load	Residual
	In	in
Gen1 Test Data	3.06	0.22
Ansys Model	3.02	0.51
Percent Error	1.6%	57.4%
Gen2 Test Data	3.38	0.17
Ansys Model	3.25	0.71
Percent Error	4.0%	75.6%

Both generation containers measured data satisfy the test residual requirements of no more residual deflection than 0.28 in. The Gen1 container resulted in a 1.6% error while under the full test load, which is inside the acceptable engineering prediction range of 5%. While the residual deflection had a 57.4% error which is off by 0.29 in and does not satisfies the test residual requirements. The Gen2 container was with the acceptable range with 4.0% error during the full test load. While the predicted residual deflection is 0.43 in over the test residual requirement. Figure 41 shows the mid-span Gen2 test and Ansys load versus pressure data are plotted. See Table A 1 row 16 for graph data. The graph shows the Ansys model stiffening under half the maximum load, thus not reaching the test data maximum deflection and resulting in more residual deflection.



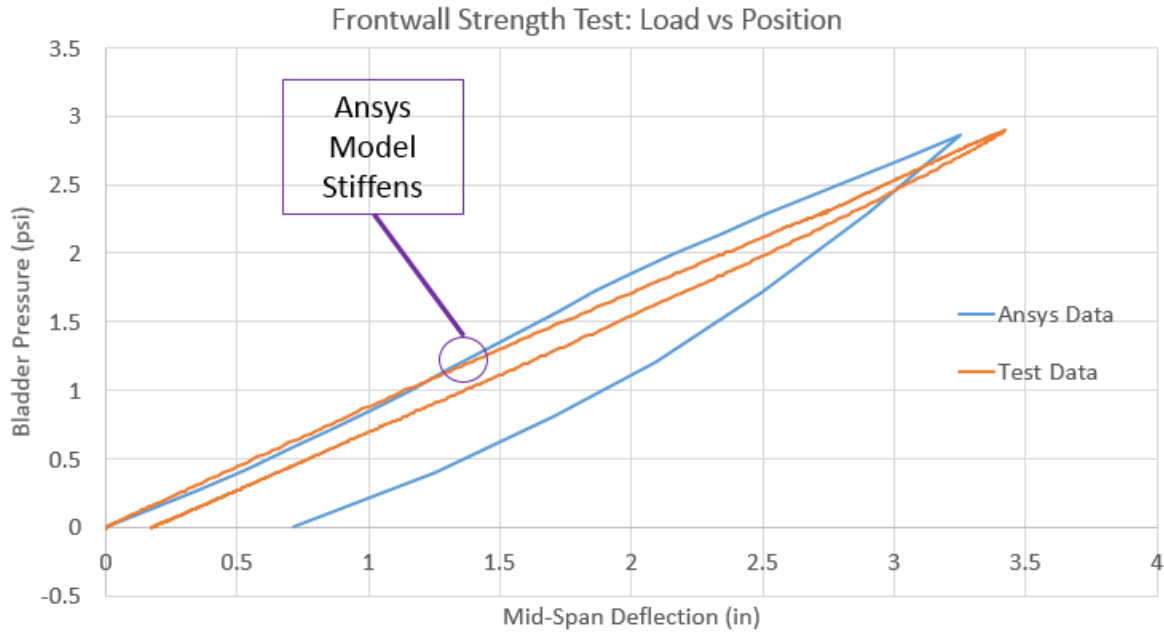


Figure 41: Frontwall Strength Test: Load vs Position Graph, at Mid-Span

Table 15 compares the strain data between the test and model for Gen1 and Gen2 containers.

Gauge 5 is oriented vertically to capture the global bending, while gauge 4 is oriented horizontal to capture their local bending aspects.

Table 15: Comparison of Frontwall Strength Test Strains

Container	Strain Gauge ( $\mu\epsilon$ )	
	4	5
Gen1 Test Data	-258	-2057
Ansys Model	251	-1946
Percent Error	203%	6%
Gen2 Test Data	-649	-2669
Ansys Model	437	-2249
Percent Error	249%	19%

Gauge 5 captures the global bending for Gen1 with 6% error and 19% error for Gen2. Gauge 4 captures the local bending of the panel edge with over 200% error for both generations, however, the magnitude is close but the model predicts tension instead of compression.

#### **4.4.3 Modeling Conclusions**

The frontwall model accurately captures the full test load represents, the Gen2 test data is under predicted by 4.0% error. The frontwall model does not accurately capture the residual deflection behavior. For Gen2 the container passes the ISO requirements with 0.1 in to spare, while it is predicted to fail by 0.43 in. The Gen2 global bending strain is captured within 19% error. The local bending strain of the panel edge is predicted in tension, while the measured strain is in compression. The frontwall model's geometry is limited. It does not include the connected sidewall, roof and floor systems, thus the model is very sensitive to its BC. This allows the model to have be computationally efficient at the cost of capturing the residual and panel edge behavior.

#### **4.5 Lifting From Fork-Lift Pockets Test**

The lifting from fork-lift pockets test was determined to be a key structural response due to prior University of Maine testing, which showed the steel tab debonding from the sidewalls, thus making the container fail ISO requirements. For convenience the test will be called fork pocket test. Summarizing from the ISO 1496-1 fork pocket test section, the test must be conducted if the container have fork-lift pockets. The test requires a uniformly distributed load over the floor, such that the combined mass of the container and test load equals 1.6 times the containers rating. The container must be supported by a 7.9 in by 80.0 in supports inserted into each fork-lift pocket and centered. This test simulates the container being lifting by a forklift. After the test, the container cannot have permanent deformations or abnormalities which render its unsuitable for use. The test setup is shown in Figure 42. See Table A 1 row 23 for test data.



Figure 42: Fork Pocket Test Setup

String pots are not shown in Figure 42, but their locations are shown on the test schematic in Figure 43. Strain gauges are not shown in Figure 42, refer to Figure 22 for locations.

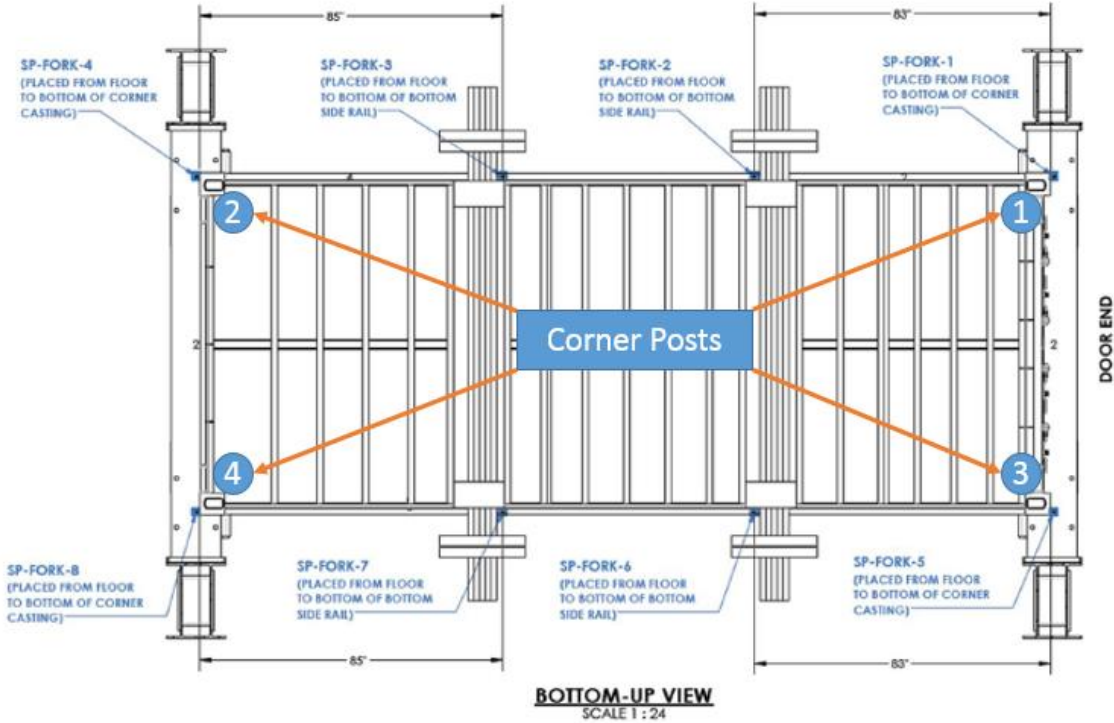


Figure 43: Fork Pocket Test String Pot Locations

The test was conducted by loading the container with concrete blocks in the same way as the previous tests and inserting the supports into the fork-lift pockets. Then the container was lifted and the supports were braced. The container was set on the supports to simulate it being lifted by the supports. Finally, the process was reversed to get the container on the ground and the concrete blocks unloaded. The schematic for the supports are shown in Figure 44.

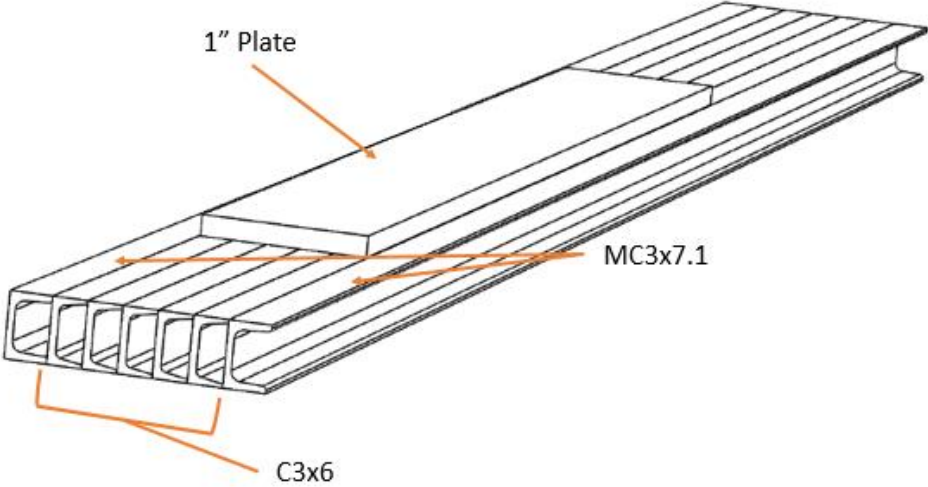


Figure 44: Fork Pocket Test Fixtures

#### 4.5.1 Development of Ansys Fork Pocket Lift Test Model

Since the sidewall model is almost a complete container model and has similar loading conditions it was modified for the fork pocket test. Throughout the modeling process of the test, two model versions were created. For Version 1, the floor geometry above the fork-lift pockets were sectioned to match the test supports contact area. The sidewall bladder load was removed and the concrete block load was adjusted to the proper magnitude for the fork pocket test load. Figure 45 shows the BC, load on the floor and bottom side rails, however, the sidewalls, roof, top side rails and corner posts are not shown to present BC and load at a better angle.

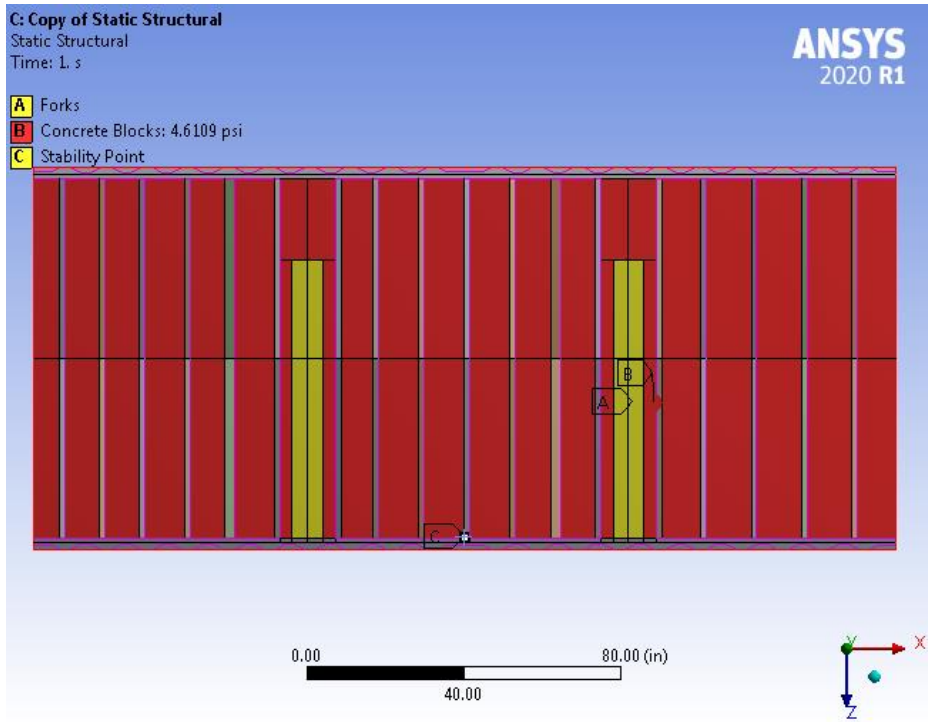


Figure 45: Fork Pocket Test Version 1 BC

The load is applied to the red and yellow rectangles. However, the yellow rectangles also represent the test supports and fix Y-displacement. BC 'B' is applied to one node in the center of the floor edge, which is fixed in the X-direction and Z-direction to stabilize the model. Figure 46 shows a deflection contour plot.

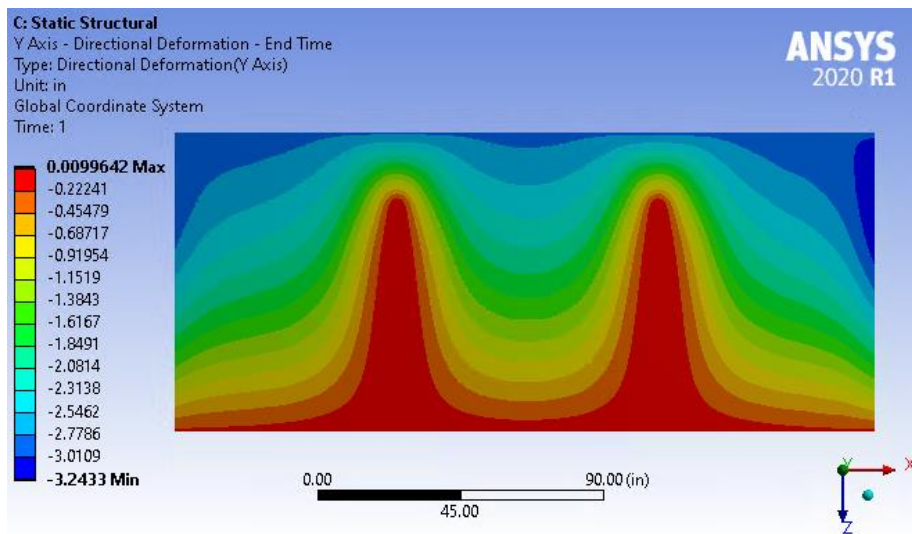


Figure 46: Version 1 Y-Deflection Contour Plot

This plot shows that the BC are too stiff because the test fixtures bow during the test, while the Ansys supports do not. The plot also shows that the floor ends are not stiff enough. Thus, Version 2 was created.

To capture the bowing test fixtures, the test fixtures were modeled. To insert the modeled fixtures, the bottom side rails had fork-lift pockets cut out. Then the fixtures were inserted, centered and connected to the contact area from Version 1. The door sill and frontwall sill were modeled, positioned then the floor was extended to the sills. A flat plate connecting the door end corner posts was modeled and given the door panel material properties from the door three-point bending test. Another flat plate connecting the front corner posts was modeled and given the frontwall panel material properties from the frontwall three-point bending test. Version 2 is the will be called the fork pocket model and is shown in Figure 47. The model has 1,339,632 eight node quadratic shell elements. See Table A 1 row 24 for Ansys files.

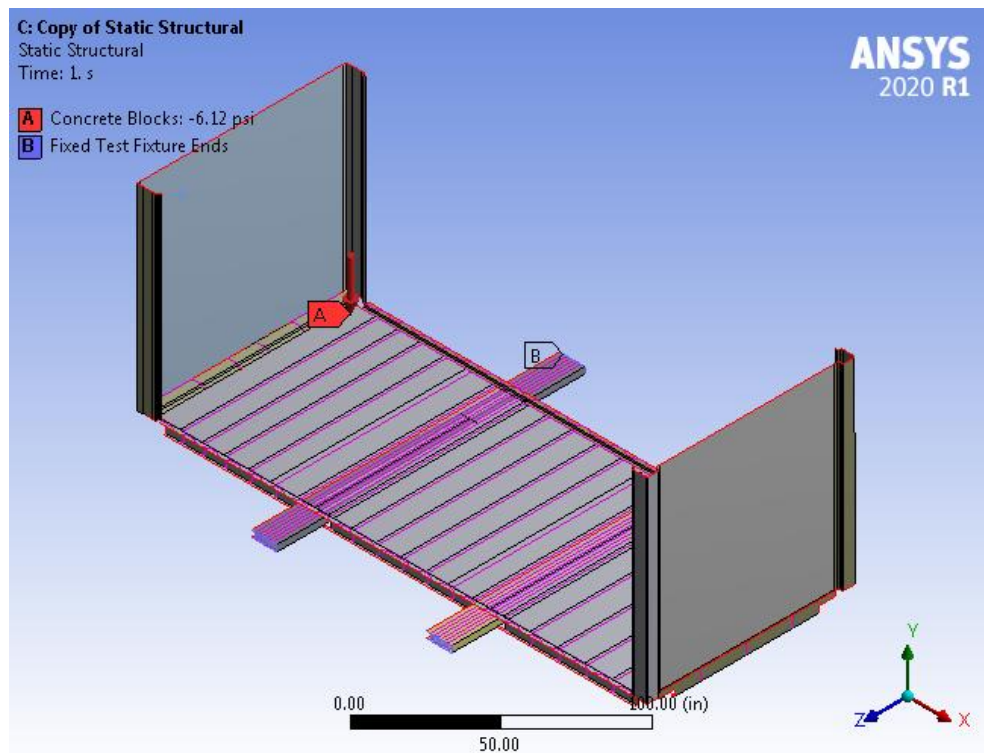


Figure 47: Fork Pocket Test Version 2 BC

#### 4.5.2 Comparison of Full-Scale Test Data to Ansys Data

Only Gen2 layups considered during comparison because the Gen2 layups were finalized before the modeling process began for the fork pocket test. No mesh study was conducted because the model was based on the verified sidewall model. No permanent deformation occurred. Loaded deflection data is compared in Table 16 and strain data in Table 17. All present errors are outside of the acceptable range, but relative to the 240 in span of the containers length a one to two millimeter variability is acceptable. See Table A 1 row 25 for comparison data.

Table 16: Comparison of Fork Pocket Test Corner Post Deflection

Container	Corner Post Deflection (in)			
	1	2	3	4
Gen2 Test Data	0.126	0.047	0.126	0.087
Ansys Model	0.169	0.083	0.185	0.083
Percent Error	24%	40%	31%	7%

All present errors are outside of the acceptable range, but relative to the 240 in span of the containers length a one to two millimeter variability is acceptable.

Table 17: Comparison of Fork Pocket Test Strains

Container	Strain Gauge ( $\mu\epsilon$ )						
	9	10	14	16	17	18	19
Gen2 Test Data	-82	24	-52	73	57	312	-897
Ansys Model	-59	34	-34	431	690	381	-1345
Percent Error	39%	29%	53%	157%	83%	92%	18%

All present errors are outside of the acceptable range, but the model predicts where the container will be in tension and compression correctly. Gauges 9, 10 and 14 capture the central bending of the sidewall within a few dozen microstrain. Gauges 16 and 17 are directly above the test fixtures and located around several components joining, which makes the strain gradient large. Gauge 18 is on a corrugation peak above the test fixture and is predicted within 70 microstrain. Gauge 19 is in a corrugation valley above the test fixture, but is not predicted within an acceptable microstrain value.

### **4.5.3 Modeling Conclusions**

Modeling the test fixtures as BC allowed for faster run times and used less computer memory. However, the BC did not capture the bowing effect which occurred in fixtures during the test. Thus modeling the fixtures was crucial for accurately capture the containers test behavior. Along with modeling the sills, door plate and frontwall plate were a crucial components in capturing the correct floor behavior. The fork pocket model predicts the corner post deflections within 0.06 in. The model accurately captures the tension and compression sections of the container during the test.



## CHAPTER

### 5 CONCLUSIONS AND POTENTIAL IMPLEMENTATIONS

#### 5.1 Conclusions

This thesis presents the development of FEA models for a hybrid composite-steel shipping container undergoing ISO structural testing. The objectives of this research were to develop layered laminate mechanical models, corrugated composite panels FEA models and full-scale ISO structural testing models and identify which modeling techniques are required to accurately predict structural behavior during ISO testing.

Laminate mechanical models were developed in VectorLam and matched to coupon testing for Gen1 and Gen2 laminate layups. Door, roof, sidewall and frontwall corrugated panels were modeled as layered shell models with three-point bending test BC and load conditions. The models were compared to measure three-point bending test data, for model verification. Steel coupon tensile tests were conducted to collect the non-linear material property data for Ansys and verified that non-linear geometry needs to be turned on to predict the structural behavior.

Full-scale models were developed for the ISO sidewall strength test, roof strength test, frontwall strength test and fork pocket test. A model technique developed during the creation of the sidewall strength test model was breaking down the structural tests into steps through model versions that developed from the previous. Linear materials and linear geometry were used during the development process to save time verifying components, while non-linear materials and non-linear geometry were used when predicting data for comparison to measured data. The roof strength test model was developed from the sidewall model by changing the loading conditions. The frontwall model underwent the same development process as the sidewall model. The fork pocket model was developed from the sidewall model by changing the loading

conditions and adding additional container components to capture the containers test behavior. The sidewall, frontwall and fork pocket models accurately capture the full test load behavior. The sidewall and frontwall model do not accurately capture the residual deflection and this needs to be further investigated. The roof model was vice versa, it accurately captured the residual deflection, but did not accurately capture the full test load behavior. The developed FEA models overall capture key components of the ISO 1496-1 testing if non-linear material modeling and non-linear geometric capability is enabled.

## **5.2 Potential Implementations**

The developed models can be used to further refine the hybrid composite-steel shipping container design. Querying high stress values on the composite-steel bond can be used to refine the bond length around each panel. Each model can be scaled up to match containers such as, 1AA and 1AAA.

The models can be used to evaluate other container designs including material substitutions, container size change to 40ft, or other alterations.

## REFERENCES

- 20FT. Containers. (n.d.). Newark, NJ, USA.
- Bakewell, J. (2019). Creating Strong Bonds. *Automotive Manufacturing Solutions*.
- Biancolini, M. (2005). Evaluation of Equivalent Stiffness Properties of Corrugated Board. *Composite Structures*, 322-328.
- Hyer, M. W. (2009). *Stress Analysis of Fiber-Reinforced Composite Materials*. Lancaster, Pennsylvania: DEStech Publications.
- Material, A. S. (2010). *ASTM E8-04 Standard Test Methods for Tension Testing of Metallic Materials*.
- Material, A. S. (2014). *ASTM D3039/D3039M-08 Standard Test Method for Tensile Properties of Polymer Matrix Composites*.
- Organization, I. S. (1996, 2005, 2007). *ISO/TR 15070*.
- Organization, I. S. (2013). *ISO 1496-1*.
- Organization, I. S. (2013). *ISO 668*.
- Snape, T. (2021). Sidewall Bending Test Schematic.
- Vectorply. (n.d.).
- Viselli, A. (2006). *Marine Composite Freight Containers: Structural Modeling and Testing*.
- Whitney, J. M. (1987). *Structural Analysis of Laminate Anisotropic Plates*. Lancaster, Pennsylvania: Technomic Publishing Company.

## APPENDIX A: ATTACHMENTS

Table A 1: File directory for attachments

Table Row	File Name	Description	Filepath
1	Container Drawings	Folder Contains Container and Test Setup Drawings	\\Jason Nagy Thesis Materials
2	Laminate Comparison Gen1	Gen1 VectorLam Outputs	\\Jason Nagy Thesis Materials\Chapter 2
3	Laminate Comparison Gen2	Gen2 VectorLam Outputs	\\Jason Nagy Thesis Materials\Chapter 2
4	Chap2 Tables	Tables used in Chapter 2	\\Jason Nagy Thesis Materials\Chapter 2
5	Gen1 Laminate Test Summary	Gen1 Coupon Test Outputs	\\Jason Nagy Thesis Materials\Chapter 2\Coupon Tests
6	Coupon Laminate Information	Gen2 Coupon Laminate Layups and Panel Weights	\\Jason Nagy Thesis Materials\Chapter 2\Coupon Tests\Gen2
7	Gen2 Laminate Test Summary (1)	Gen2 Roof, Frontwall and Sidewall Coupon Test Outputs	\\Jason Nagy Thesis Materials\Chapter 2\Coupon Tests\Gen2
8	Gen2 Laminate Test Summary (2)	Gen2 Roof and Door Coupon Test Outputs	\\Jason Nagy Thesis Materials\Chapter 2\Coupon Tests\Gen2
9	Chap3 Tables	Tables used in Chapter 3	\\Jason Nagy Thesis Materials\Chapter 3
10	Full Panel Bending Test Models	Folder Contains Ansys Models for All Panel's Three-Point Bending Tests	\\Jason Nagy Thesis Materials\Chapter 3\Full Panel Bending Test Models
11	Chap4 - Steel Coupon	Data Used for Steel Coupon Test Section	\\Jason Nagy Thesis Materials\Chapter 4\Steel Coupon
12	Steel Coupon Test Model	Folder Contains Ansys Model for Steel Coupon Test	\\Jason Nagy Thesis Materials\Chapter 4\Steel Coupon\Ansys Model
13	Sidewall Test Data	Folder Contains Sidewall Test Data for Gen1 and Gen2	\\Jason Nagy Thesis Materials\Chapter 4\Sidewall\Sidewall Test Data
14	Sidewall Test Model	Drive Contains Ansys Model for Sidewall Test	Shared Google Drive: Jason Nagy Thesis Materials
15	Chapter 4 - Sidewall	Tables Used for Sidewall Test Section	\\Jason Nagy Thesis Materials\Chapter 4\Sidewall
16	Load vs Mid-Span Deflection Graphs	Load vs Mid-Span Deflection Graphs for the Sidewall, Frontwall Tests	\\Jason Nagy Thesis Materials\Chapter 4
17	Roof Test Data	Folder Contains Roof Test Data for Gen1 and Gen2	\\Jason Nagy Thesis Materials\Chapter 4\Roof\Roof Test Data

Table A 1 Continued

18	Roof Test Model	Drive Contains Ansys Model for Roof Test	Shared Google Drive: Jason Nagy Thesis Materials
19	Chapter 4 - Roof	Tables Used for Roof Test Section	\\Jason Nagy Thesis Materials\Chapter 4
20	Frontwall Test Data	Folder Contains Frontwall Test Data for Gen1 and Gen2	\\Jason Nagy Thesis Materials\Chapter 4\Frontwall\Frontwall Test Data
21	Frontwall Test Model	Drive Contains Ansys Model for Frontwall Test	Shared Google Drive: Jason Nagy Thesis Materials
22	Chapter 4 - Frontwall	Tables Used for Frontwall Test Section	\\Jason Nagy Thesis Materials\Chapter 4
23	Gen2 Fork Pocket Test Data	Gen2 Fork Pocket Test Data	\\Jason Nagy Thesis Materials\Chapter 4\Fork Pocket
24	Fork Pocket Test Model	Drive Contains Ansys Model for Fork Pocket Test	Shared Google Drive: Jason Nagy Thesis Materials
25	Chapter 4 - Fork Pocket	Tables Used for Fork Pocket Test Section	\\Jason Nagy Thesis Materials\Chapter 4\Fork Pocket

## APPENDIX B: THREE-POINT BENDING TEST PLOTS

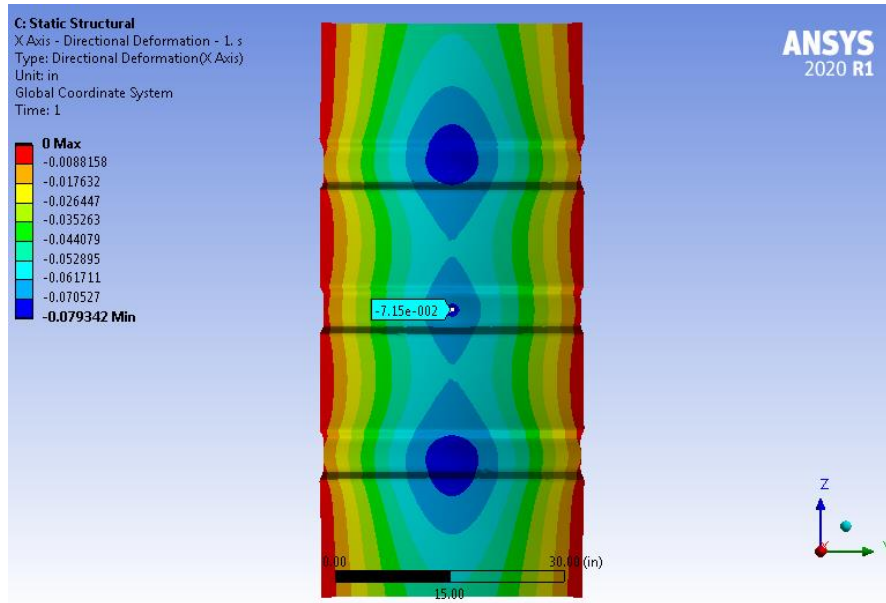


Figure B 1: Door Panel Deflection Contour Plot

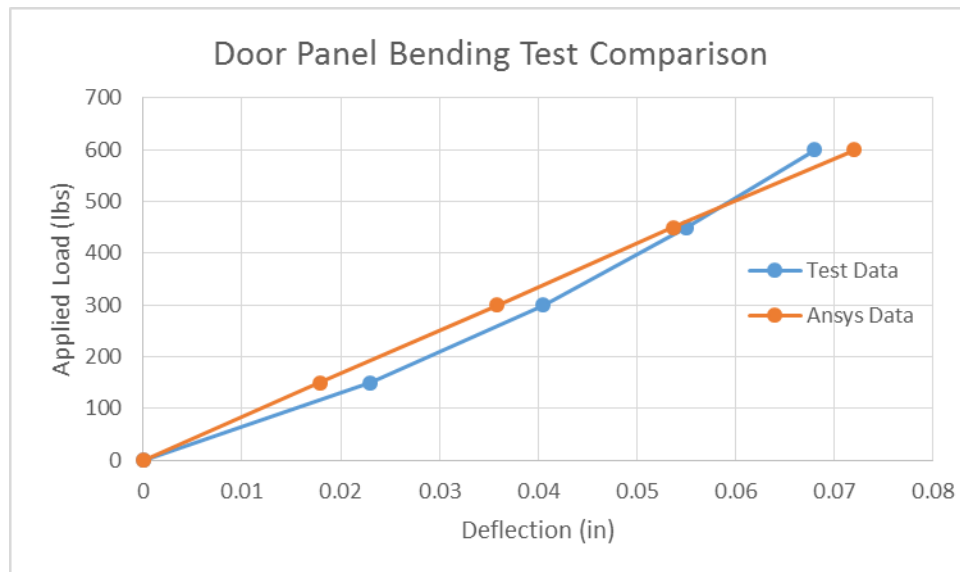


Figure B 2: Comparison of Door Panel Bending Test Data

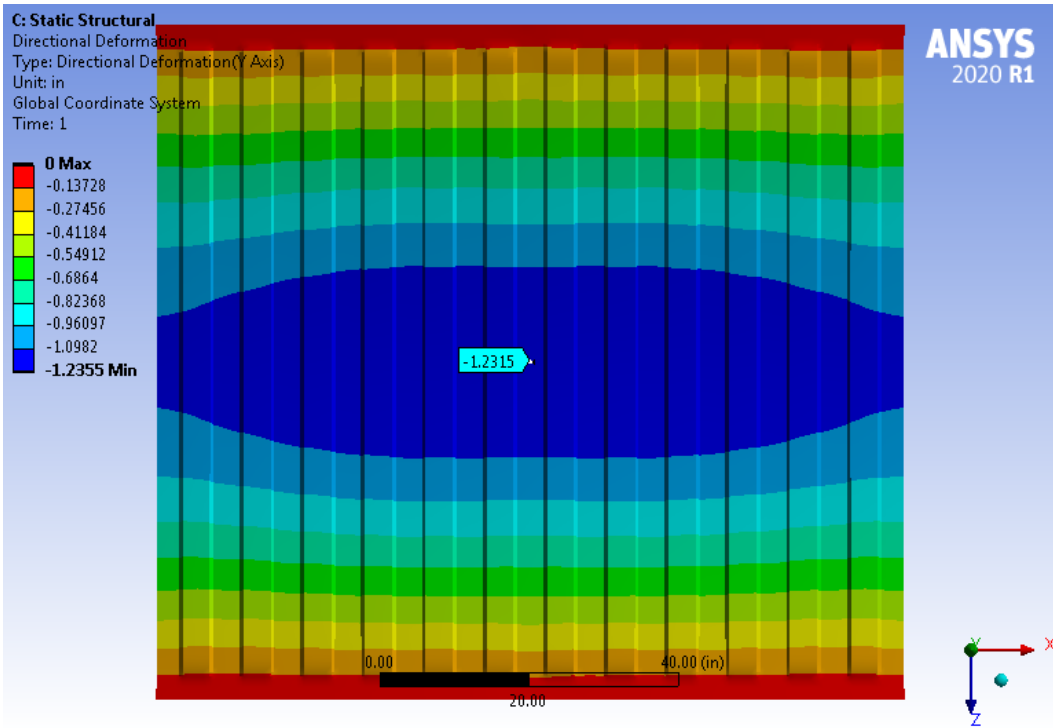


Figure B 3: Roof Panel Deflection Contour Plot

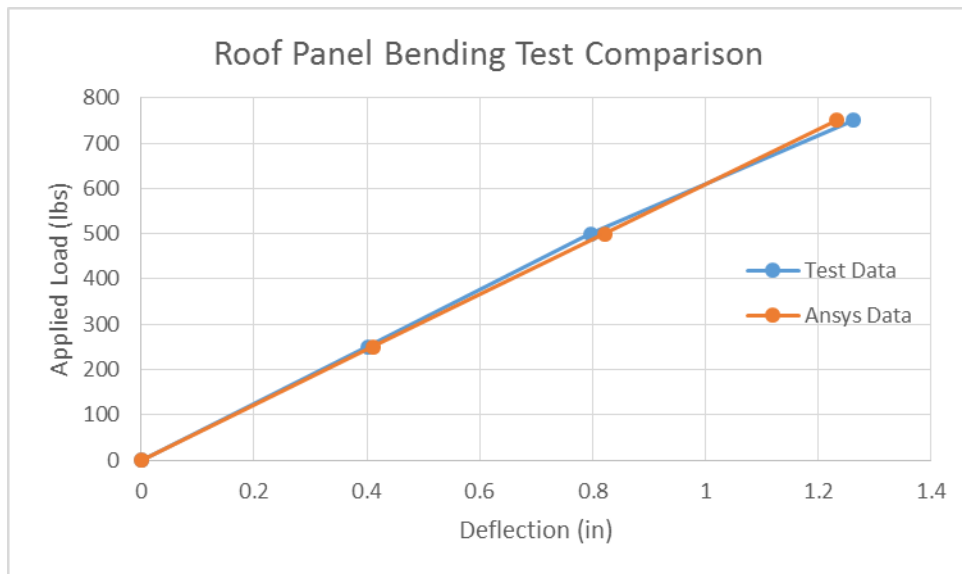


Figure B 4: Comparison of Roof Panel Bending Test Data

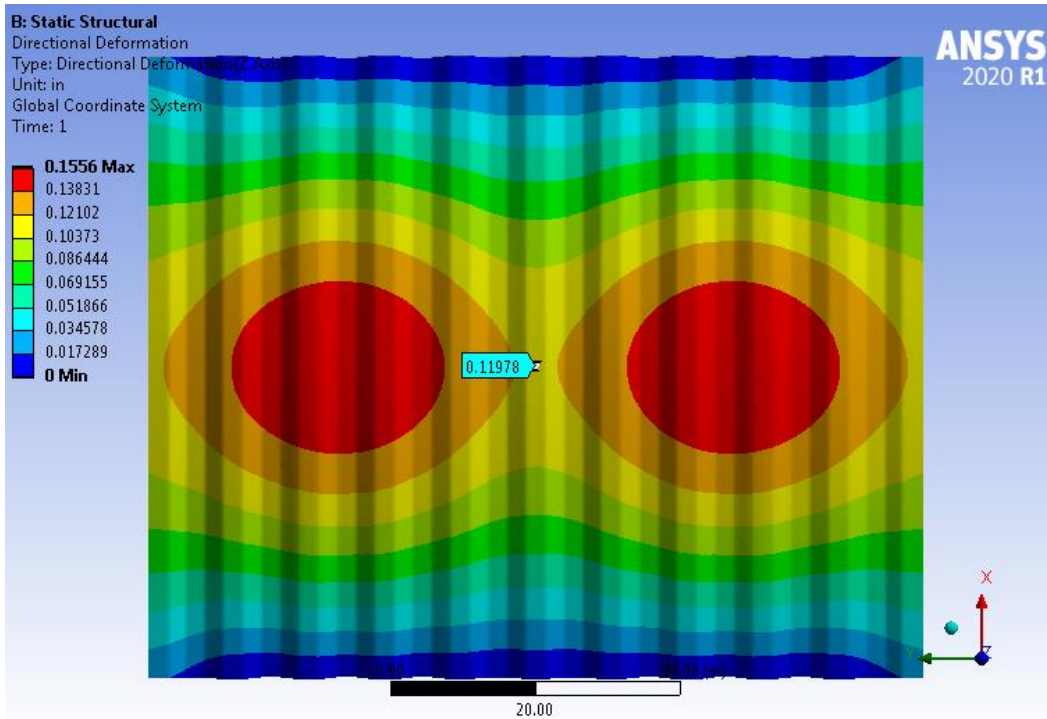


Figure B 5: Sidewall Panel Deflection Contour Plot

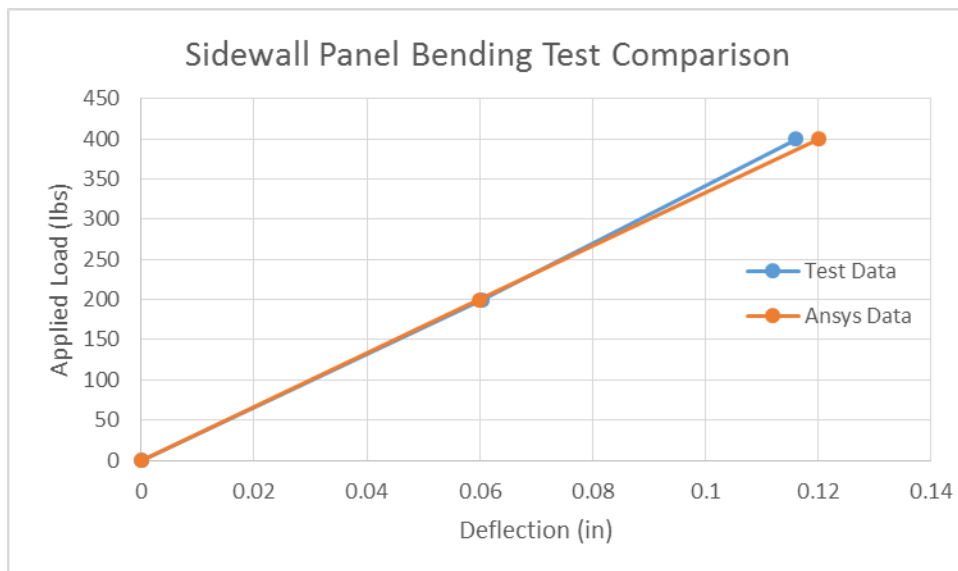


Figure B 6: Comparison of Sidewall Panel Bending Test Data



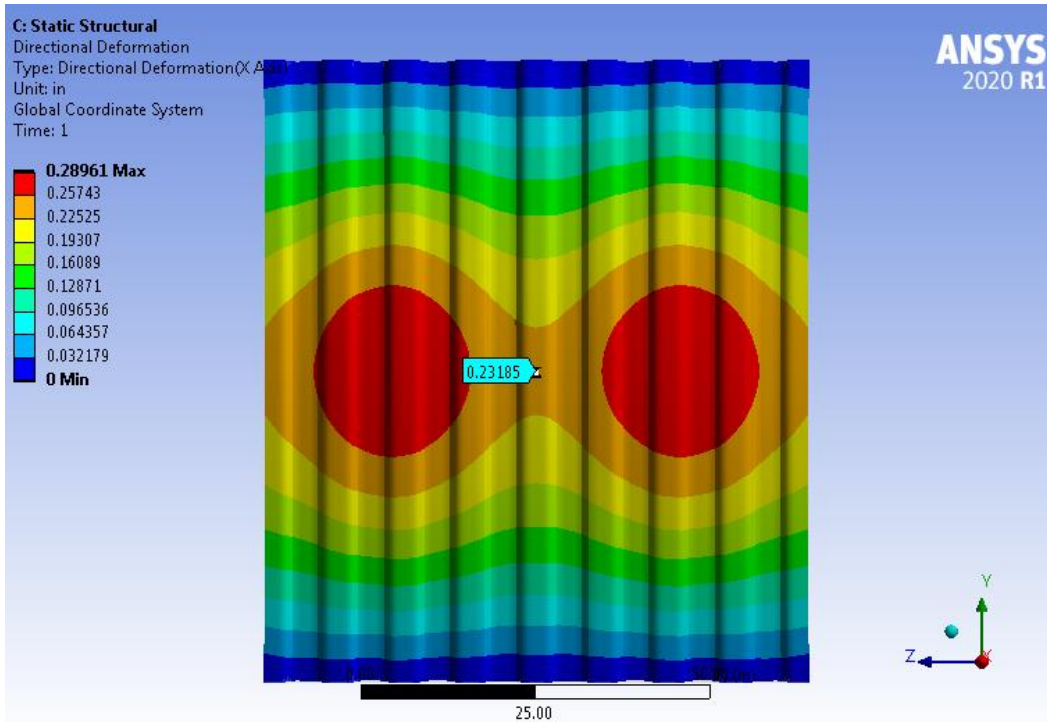


Figure B 7: Frontwall Panel Deflection Contour Plot

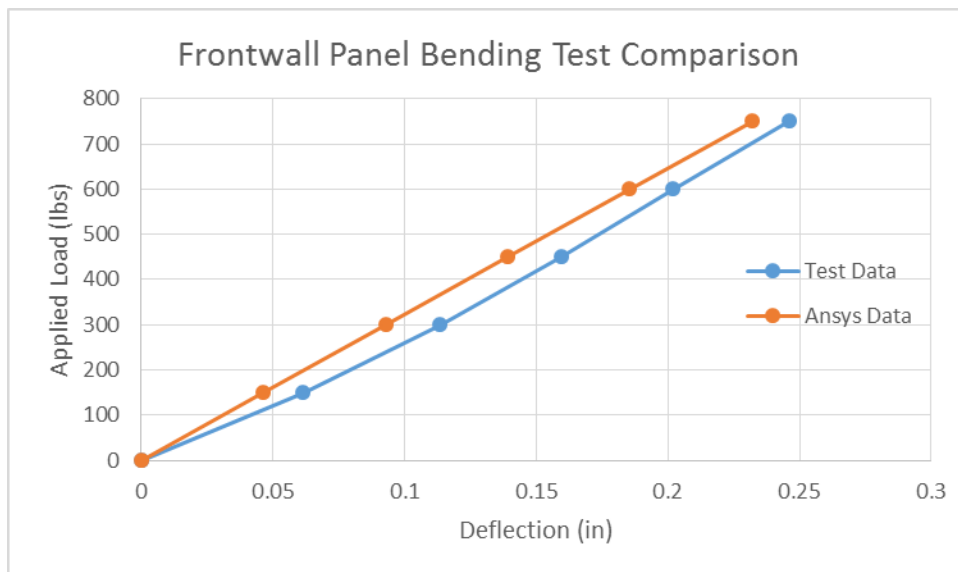


Figure B 8: Comparison of Frontwall Panel Bending Test Data

## **BIOGRAPHY OF THE AUTHOR**

Jason Nagy was born in Bridgeport, Connecticut on November 27, 1998. He was raised in Gorham, Maine and graduated from Gorham High School in 2016. He attended the University of Maine and graduated in 2020 with a Bachelor's degree in Mechanical Engineering. He entered the Mechanical Engineering graduate program at The University of Maine in the fall of 2020. After receiving his degree, Jason will be joining the University of Maine Advanced Structures and Composites Center, to begin his career in the finite element modeling. Jason is a candidate for the Master of Science degree in Mechanical Engineering from the University of Maine in May 2022.